Autonomous cooperative formation control of underactuated USVs based on improved MPC in complex ocean environment

Zaopeng Dong[*a,b,c,d], Zhengqi Zhang[a,c], Shijie Qi[a,c], Haisheng Zhang[a,c], Jiakang Li[a,c] ,

Yuanchang Liu[d]

a Key Laboratory of High Performance Ship Technology (Wuhan University of Technology), Ministry of Education, Wuhan University of Technology, China

b Science and Technology on Underwater Vehicle Laboratory, Harbin Engineering University, China

c School of Naval Architecture, Ocean and Energy Power Engineering, Wuhan University of Technology, China

d Department of Mechanical Engineering, University College London, London, UK

Abstract. A dual model predictive control (DMPC) method based on virtual trajectory is proposed in this paper, in order to achieve autonomous cooperative formation control of underactuated unmanned surface vehicles (USVs) in complex ocean environment. Firstly, the formation tracking error model of the USVs is designed, and considering the large initial state tracking error of USVs, a virtual transition trajectory is put forward to guide the design of tracking controller. To solve the mutation problem caused by misalignment of the follower USV's desired trajectory in the early stage, an improved differential tracker is introduced into virtual leader USV to smooth the desired trajectory of the follower USV. In addition, a dual mode switching strategy is designed to decide when and how to quit the transition of the virtual USV. A nonlinear disturbance observer is introduced to compensate the complex marine environment interference. Finally, by introducing terminal penalty function and linear state feedback controller, the Lyapunov function is constructed to prove the control stability of the proposed model predictive control method in finite time domain, and

Corresponding Author: Zaopeng Dong, E-mail: dongzaopeng@whut.edu.cn

the effectiveness and reliability of the proposed method are verified by simulation experiments.

Key words: Unmanned surface vehicle (USV); leader-follower; cooperative formation control; model predictive control (MPC); virtual transition trajectory;

ARTICLE INFO. Handling Editor: Prof. A.I. Incecik

1. Introduction

Unmanned surface vehicles (USVs) play an increasingly important role in marine activities, such as ocean resources exploration, maritime casualty search and reconnaissance (Krell et al., 2022; Makar, 2022; Rodriguez et al., 2022; Baek and Woo, 2022; Patterson et al., 2022). Compared with the single USV, a coordinated group of USVs is more capable and flexible of performing complicated tasks (Lindsay et al., 2022; Solnør et al., 2022). As an enabling technology of these applications, the autonomous cooperative formation control of a group of underactuated USVs has received considerable attention recently (Azarbahram et al., 2022). One core problem concerned with the multi-USV system is the formation tracking control which requires the USVs to keep a prescribed formation while tracking a given reference trajectory simultaneously (Martinsen et al., 2022; MahmoudZadeh et al., 2022). A number of related research works have been carried out on the formation tracking control of USV, and many valuable research results have been published.

A robust control algorithm is developed for time-varying formation of multiple underactuated autonomous underwater vehicles (AUVs) with disturbances under input

Corresponding Author: Zaopeng Dong, E-mail: dongzaopeng@whut.edu.cn

saturation by Li et al. (2019), and leader-follower formation control problem of multiple underactuated AUVs under uncertain dynamics and limited control torques is addressed in (Wang et al., 2020), where a multi-layer neural network-based estimation model is designed to handle the unknown follower dynamics. Implementation of a potential field algorithm for formation control of a swarm of low-cost unmanned surface vehicles is discussed by Bhanderi and McCue (2020) and the goal of their work is to extend this established approach for ground vehicles to maritime surface vessels. The article (Wang et al., 2019) investigates the leader-follower formation control of underactuated AUVs with model uncertainties and external disturbances, where sliding mode control, multilayer neural network, and adaptive robust techniques are employed to design a formation controller. A multiple AUV control strategy is introduced by Chen et al. (2020) to improve the cooperative operation ability in formation control and cluster search operations, and to minimize the likelihood of collisions and interference with teammates and obstacles under various complex working conditions. The problem of formation autonomous navigation system (FANS) for USVs is discussed by Sun et al. (2020), where the decision layer of the system is composed of path planning subsystem and navigation control subsystem to realize fast and effective autonomous navigation system. Formation control problem of multiple AUVs in the presence of model uncertainties and ocean-current disturbances is addressed by Meng and Zhang (2021), and a robust distributed leaderless formation control strategy, integrated by a cross-coupling

Corresponding Author: Zaopeng Dong, E-mail: dongzaopeng@whut.edu.cn

synchronous control technique, a nonsingular terminal sliding-mode control approach, and an adaptive control method, is proposed.

A novel distributed guidance system is established (Liu et al., 2021) based on leader-follower strategy, by using a portion of communication links to simplify the formation control design, and an event-triggered formation strategy based on fixed-time Radial Basis Function(RBF) neural network adaptive disturbance observer is proposed in literature (Wang and Su, 2021), which can ensure formation control converge in fixed time. A distributed Lyapunov-based model predictive controller (DLMPC) is designed in (Wei et al., 2019) and the AUVs can keep the desired formation while tracking the reference trajectory, despite the presence of external disturbances. A distributed prescribed performance control strategy is put forward for three-dimension (3D) time-varying formation of multiple underactuated AUVs with uncertain dynamics and unknown disturbances in (Li et al., 2021), where a novel form of prescribed performance function is proposed, so that the desired time, needed for the AUVs' formation tracking errors to reach and stay within the prescribed tolerant band, can be preset exactly and flexibly. Dynamic event-triggered mechanism (DETM) formation control method based on adaptive fixed time integral sliding mode disturbance observer (AFISMDO) is proposed by Su et al. (2021), which not only can ensure formation control converge in fixed time, but also can further reduce the consumption of the controller network transmission. Finite-time distributed formation control for USVs exposed to external disturbances, model uncertainties and input

Corresponding Author: Zaopeng Dong, E-mail: dongzaopeng@whut.edu.cn

saturation constraints is addressed by Huang et al. (2021), and by combing the sliding mode control method and adaptive algorithms, two control architectures are developed for USVs' formation control problem. Multi-AUV formation trajectory tracking control methods in the case of weak communication environment under discrete-time collection are discussed in (Yan et al. 2022), and in light of the sliding mode control (SMC) approach, concerns the formation regulation for a network of unmanned surface vehicles (USVs) with environmental disturbances,the formation pattern is configured within the consensus-based leaderless framework by Jiang and Xia (2022).

MPC is a multivariate control strategy and could deal with various constraints on spatial state variables. Also it is widely used in basic motion control such as speed and heading control (Wang and Liu, 2021; Zhang et al., 2019; Jimoh et al., 2021), path following (Liu et al., 2020a; Yao et al.,2020; Liu et al., 2020b; Zeng et al., 2020; Li et al., 2021; Liang et al., 2020b; Codesseira and Tannuri, 2021; Sandeepkumar et al., 2022), trajectory tracking (Shen et al., 2017; Shen and Shi 2020; Yang et al., 2020; Kong et al., 2020; Liang et al., 2020a) and formation control (Liu et al., 2021; Wei et al., 2019) of unmanned marine vehicles.

Up to now, the MPC control algorithm for a single ship has been studied in many papers, but its application to formations remains very rare. In practical USV applications, system limitations such as thrust limits and safe work zones are unavoidable. Therefore, these constraints need to be considered during the tracking

Corresponding Author: Zaopeng Dong, E-mail: dongzaopeng@whut.edu.cn

controller design process. But few other existing control methods take these into account, and MPC has a natural advantage in dealing with this aspect. Based on the above considerations, a dual MPC control method is designed in this paper to solve the unmanned ship formation control problem. The controller is improved with respect to the large amount of starting state deviation, which leads to actuator over-tuning, and the sudden change in the amount of target state due to the expected trajectory not being smooth in the early stage. The main innovations of the paper are: (1) A dual model predictive control method based on virtual USV trajectory is proposed for the cooperative formation control of USVs. (2) An improved differential tracker is introduced into virtual leader USV to smooth the desired trajectory of the follower USV. (3) A dual-mode switching strategy is designed to select the virtual trajectory or the desired trajectory as the USVs' tracking trajectory.

The subsequent papers are scheduled as follows: After the introduction, the ship model, formation generation and control objective are presented in Chapter 1. In Chapter 2, the formation controller is designed, containing the dual MPC control based on virtual USV, formation desired trajectory smoothing, and nonlinear disturbance observer. The stability proofs of the observer and controller are provided in Chapter 3. Then, three conditions are designed in Chapter 4 to perform simulation analysis. Finally, the conclusions are presented in Chapter 5.

2. Model and problem statement

In this paper, formation control algorithms for multiple USVs are proposed. And

Corresponding Author: Zaopeng Dong, E-mail: dongzaopeng@whut.edu.cn

the kinematic model of the USV and statement of the formation problem are introduced in this section. The leader–follower formation method is adopted for the design of cooperative formation control law for USVs, as shown in Figure 1.

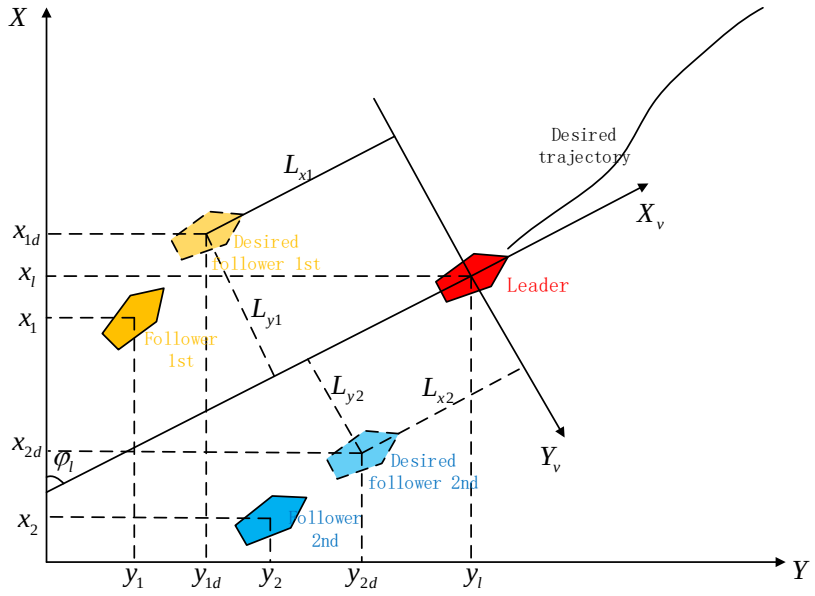

Figure 1. Formation Control Diagram

Combined with Figure 1, it can be seen that the formation control problem can be described as tracking control of the desired trajectory by the leader and tracking control of the desired position by the followers. Next, the USV models will be built and the form of the desired position of the follower is generated.

2.1. System models

Assuming that the formation consists of N USVs, according to the literature (Perez and Fossen, 2007), the kinematic model of the i^{th} $(i=1,2,\cdots N)$ USV can be represented as:

$$\dot{\boldsymbol{\eta}}_i = \boldsymbol{R}(\varphi_i)\boldsymbol{v}_i \tag{1}$$

Where $\boldsymbol{\eta}_i = \begin{bmatrix} x_i & y_i & \varphi_i \end{bmatrix}^T$ is the position and heading vector of the i^{th} USV;

Corresponding Author: Zaopeng Dong, E-mail: dongzaopeng@whut.edu.cn

x_i is the longitudinal position of the i^{th} USV; y_i is the lateral position of the i^{th} USV; φ_i is the bow angle of the i^{th} USV; $\boldsymbol{v}_i = \begin{bmatrix} u_i & v_i & r_i \end{bmatrix}^T$ is the velocity vector of the i^{th} USV; u_i is the longitudinal velocity of the i^{th} USV; v_i is the lateral velocity of the i^{th} USV; r_i is the bow angle speed of the i^{th} USV; $\boldsymbol{R}(\varphi_i)$ is the standard rotation matrix of the i^{th} USV, defined as

$$\boldsymbol{R}(\varphi_i) = \begin{bmatrix} \cos(\varphi_i) & -\sin(\varphi_i) & 0 \\ \sin(\varphi_i) & \cos(\varphi_i) & 0 \\ 0 & 0 & 1 \end{bmatrix}.$$

According to the literature (Perez and Fossen, 2007), the nonlinear dynamics model of the i^{th} USV can be expressed via laws of Newton:

$$\boldsymbol{M}_i \dot{\boldsymbol{v}}_i + \boldsymbol{C}(\boldsymbol{v}_i)\boldsymbol{v}_i + \boldsymbol{D}_i \boldsymbol{v}_i = \boldsymbol{\tau}_i + \boldsymbol{w}_i \tag{2}$$

Where $\boldsymbol{M}_i$ is the inertia matrix including added mass of the i^{th} USV. $\boldsymbol{C}(\boldsymbol{v}_i)$ denotes the Coriolis and centripetal matrix of the i^{th} USV. $\boldsymbol{D}_i$ is the hydrodynamic damping coefficient matrix mainly including drag force and vortex-induced force of the i^{th} USV. $\boldsymbol{\tau}_i$ is the generalized thrust vector of the i^{th} USV. $\boldsymbol{w}_i$ represents the external disturbances vector of the i^{th} USV. Defined as:

$$\boldsymbol{M}_i = diag(m_{1i}, m_{2i}, m_{3i}) \ , \ \boldsymbol{C}(\boldsymbol{v}_i) = \begin{bmatrix} 0 & 0 & -m_{2i}v_i \\ 0 & 0 & m_{1i}u_i \\ m_{2i}v_i & -m_{1i}u_i & 0 \end{bmatrix} \ , \ \boldsymbol{D}_i = diag(d_{1i}, d_{2i}, d_{3i}) \ ,$$

$\boldsymbol{\tau}_i = \begin{bmatrix} \tau_{ui} & 0 & \tau_{ri} \end{bmatrix}^T$, $\boldsymbol{w}_i = \begin{bmatrix} \omega_{ui} & \omega_{vi} & \omega_{ri} \end{bmatrix}^T$.

External disturbances can be compensated by MPC robustness and nonlinear disturbances observer (as will be seen in Section 2.5). Therefore, the influence of external disturbances is not considered in the controller design. Expanding the

Corresponding Author: Zaopeng Dong, E-mail: dongzaopeng@whut.edu.cn

kinematic equations (1) and the dynamic equations (2), we have

$$\begin{cases} \dot{x}_i = u_i \cos\varphi_i - v_i \sin\varphi_i \\ \dot{y}_i = u_i \sin\varphi_i + v_i \cos\varphi_i \\ \dot{\varphi}_i = r_i \\ \dot{u}_i = \dfrac{m_{2i}}{m_{1i}} v_i r_i - \dfrac{d_{1i}}{m_{1i}} u_i + \dfrac{1}{m_{1i}} \tau_{ui} \\ \dot{v}_i = -\dfrac{m_{1i}}{m_{2i}} u_i r_i - \dfrac{d_{2i}}{m_{2i}} v_i \\ \dot{r}_i = \dfrac{m_{1i} - m_{2i}}{m_{3i}} u_i v_i - \dfrac{d_{3i}}{m_{3i}} r_i + \dfrac{1}{m_{3i}} \tau_{ri} \end{cases} \tag{3}$$

2.2. Desired trajectory designed by USV formation

2.2.1. Status under reference system

With the desired trajectory (x_{id} , y_{id}) of the i^{th} USV, according to the literature (Shen and Shi, 2020), the status equation under the reference system can be derived:

$$\begin{aligned} &\varphi_{id} = \arctan 2\left(\dot{y}_{id}, \dot{x}_{id}\right), u_{id} = \sqrt{\dot{x}_{id}^{\ 2} + \dot{y}_{id}^{\ 2}} \\ &v_{id} = 0, r_{id} = \left(\dot{x}_{id}\ddot{y}_{id} - \dot{y}_{id}\ddot{x}_{id}\right) / \left(\dot{x}_{id}^{\ 2} + \dot{y}_{id}^{\ 2}\right) \end{aligned} \tag{4}$$

Where x_{id} is the desired longitudinal position of the i^{th} USV, y_{id} is the desired lateral position of the i^{th} USV; φ_{id} is the desired bow angle of the i^{th} USV; u_{id} is the desired longitudinal velocity of the i^{th} USV; v_{id} is the desired lateral velocity of the i^{th} USV; r_{id} is the desired bow angle speed of the i^{th} USV;

2.2.2. Formation desired trajectory

As shown in Fig.1, the location of the leader is $Y_l = \begin{bmatrix} x_l & y_l \end{bmatrix}^T$, where x_l is the longitudinal position of the leader, y_l is the lateral position of the leader. The location of the j^{th} $\left(j = 1, 2, \cdots N-1\right)$ follower is $Y_j = \begin{bmatrix} x_j & y_j \end{bmatrix}^T$, where x_j is the longitudinal position of the j^{th} follower, y_j is the lateral position of the j^{th} follower. The desired location of the j^{th} follower is $Y_j^d = \begin{bmatrix} x_{jd} & y_{jd} \end{bmatrix}^T$, where x_{jd}

Corresponding Author: Zaopeng Dong, E-mail: dongzaopeng@whut.edu.cn

is the desired longitudinal position of the j^{th} follower, y_{jd} is the desired lateral position of the j^{th} follower. The formation of the j^{th} follower is $L_j = \begin{bmatrix} L_{xj} & L_{yj} \end{bmatrix}^T$, where L_{xj} is the desired longitudinal position of the j^{th} follower in the coordinate system of the leader. L_{yj} is the desired lateral position of the j^{th} follower in the coordinate system of the leader. Combining with Figure 1, the desired position of the j^{th} follower can be expressed as:

$$Y_j^d = Y_l + R(\varphi_l) \cdot L_j \tag{5}$$

Where $R(\varphi_l)$ is the standard rotation matrix satisfying:

$R(\varphi_l) = \begin{bmatrix} \cos(\varphi_l) & -\sin(\varphi_l) \\ \sin(\varphi_l) & \cos(\varphi_l) \end{bmatrix}$, φ_l is the bow angle of the leader.

2.3. Error Model

Define $X_i = \begin{bmatrix} x_i & y_i & \varphi_i & u_i & v_i & r_i \end{bmatrix}^T$ as the states variable of actual system of the i^{th} USV, $X_{id} = \begin{bmatrix} x_{id} & y_{id} & \varphi_{id} & u_{id} & v_{id} & r_{id} \end{bmatrix}^T$ are the states variable of reference system of the i^{th} USV, $U_i = \begin{bmatrix} \tau_{ui} & \tau_{ri} \end{bmatrix}^T$ are the inputs of actual system of the i^{th} USV, $U_{id} = \begin{bmatrix} \tau_{uid} & \tau_{rid} \end{bmatrix}^T$ are the inputs of reference system of the i^{th} USV.

Then the trajectory tracking error model of the i^{th} USV can be expressed as:

$$\dot{\tilde{X}}_i = f\left(\tilde{X}_i, \tilde{U}_i\right) \tag{6}$$

Where $\tilde{X}_i = X_i - X_{id}$ are the states variable deviation of the i^{th} USV, $\tilde{U}_i = U_i - U_{id}$ are the inputs deviation of the i^{th} USV.

The aforesaid tracking problem is solved by designing a suitable control input $\tilde{U}_i$ such that $\tilde{X}_i$ tends to zero, then the USV formation is considered to keep up with the desired trajectory.

Corresponding Author: Zaopeng Dong, E-mail: dongzaopeng@whut.edu.cn

3. Controller design

3.1. Dual MPC controller design based on virtual USV

When the i^{th} USV tracks the target trajectory, the initial state variable X_i often differs significantly from the desired state variable X_{id} calculated from the desired trajectory. In the initial stage of control of USV using MPC method, there are actual situations such as actuator constraints, so it is more difficult to achieve error convergence in finite time horizon. Sharp changes will be generated in the control force and moment of the USV, which may also lead to the tracking accuracy requirements of the USV not being met, etc.

To address this phenomenon, the idea of virtual USV will be introduced before designing the dual MPC controllers in this paper. Firstly, controller 1 is designed to achieve the trajectory tracking of the virtual USV in advance, and then the state variable of the virtual USV at each time point is used as the intermediate guide state variable to replace the desired state variable of the USV, so as to get a new more gentle state variable deviation $\tilde{X}_i$, and then controller 2 is designed to achieve the trajectory tracking control of the USV. The flow of the whole controller is shown in Fig.2:

Corresponding Author: Zaopeng Dong, E-mail: dongzaopeng@whut.edu.cn

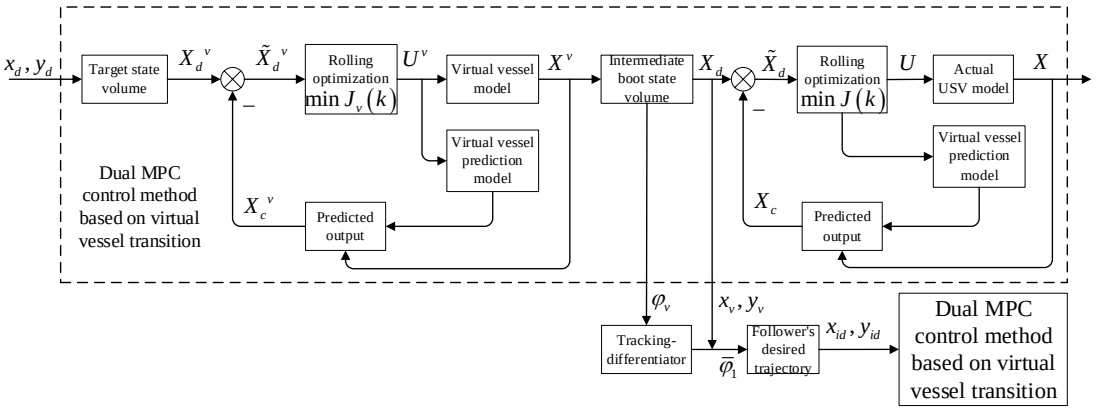

Figure 2. Flowchart of cooperative formation control for underactuated USVs

Step 1: Virtual USV establishment

A virtual USV model whose initial position coincides with the actual i^{th} USV is established. The virtual USV only plays the role of smooth transition of position information, so its dynamic model does not need to be considered, and its model can be expressed as follows:

$$\begin{cases} \dot{x}_{iv} = u_{iv}\cos\varphi_{iv} - v_{iv}\sin\varphi_{iv} \\ \dot{y}_{iv} = u_{iv}\sin\varphi_{iv} + v_{iv}\cos\varphi_{iv} \\ \dot{\varphi}_{iv} = r_{iv} \\ \dot{v}_{iv} = -\dfrac{m_{1i}}{m_{2i}}u_{iv}r_{iv} - \dfrac{d_{2i}}{m_{2i}}v_{iv} \end{cases} \tag{7}$$

Where x_{iv} is the longitudinal position of the i^{th} virtual USV, y_{iv} is the lateral position of the i^{th} virtual USV, φ_{iv} is the bow angle of the i^{th} virtual USV, u_{iv} is the longitudinal velocity of the i^{th} virtual USV, v_{iv} is the lateral velocity of the i^{th} virtual USV, r_{iv} is the bow angle speed of the i^{th} virtual USV.

Define $X_i^v = \begin{bmatrix} x_{iv} & y_{iv} & \varphi_{iv} & v_{iv} \end{bmatrix}^T$ as the states variable of actual system of the i^{th} virtual USV, $X_{id}^v = \begin{bmatrix} x_{id} & y_{id} & \varphi_{id} & v_{id} \end{bmatrix}^T$ are the states variable of reference system of the i^{th} virtual USV, $U_i^v = \begin{bmatrix} u_{iv} & r_{iv} \end{bmatrix}^T$ are the inputs of actual system of the i^{th}

Corresponding Author: Zaopeng Dong, E-mail: dongzaopeng@whut.edu.cn

virtual USV, $U_{id}^{v}=\begin{bmatrix}u_{id} & r_{id}\end{bmatrix}^{T}$ are the inputs of reference system of the i^{th} virtual USV.

Step 2: Model Linearization

In order to unify the design process of describing MPC controllers for virtual USV and actual USV, defined as $X_i^0=X_i^v$, $X_{id}^0=X_{id}^v$, $U_i^0=U_i^v$, $U_{id}^0=U_{id}^v$, $X_i^1=X_i$, $X_{id}^1=X_{id}$, $U_i^1=U_i$, $U_{id}^1=U_{id}$. Then the model used for the USV trajectory tracking control design is established as follows:

$$\dot{X}_i^a=f\left(X_i^a,U_i^a\right),\ \ i=1,2\cdots N,\ \ a=0,1 \tag{8}$$

And the MPC reference system equation is shown as:

$$\dot{X}_{id}^a=f\left(X_{id}^a,U_{id}^a\right) \tag{9}$$

Because the model of USV is a nonlinear system, in order to reduce the calculation, it needs to be approximately linearized to a linear time-varying system when designing the MPC controller. Therefore, model (8) needs to be expanded by a first-order Taylor expansion at the desired trajectory reference point $\left(X_{id}^a,U_{id}^a\right)$ as follows:

$$\dot{X}_i^a=f\left(X_{id}^a,U_{id}^a\right)+\left.\frac{\partial f}{\partial X_i^a}\right|_{\substack{X_i^a=X_{id}^a\\U_i^a=U_{id}^a}}\left(X_i^a-X_{id}^a\right)+\left.\frac{\partial f}{\partial U_i^a}\right|_{\substack{X_i^a=X_{id}^a\\U_i^a=U_{id}^a}}\left(U_i^a-U_{id}^a\right) \tag{10}$$

Combining equations (9) and (10), the linearized model of the deviation between the actual and desired state variables of the i^{th} USV is obtained as follows:

$$\dot{\tilde{X}}_i^a=A_a\tilde{X}_i^a+B_a\tilde{U}_i^a \tag{11}$$

Where $\tilde{X}_i^a=X_i^a-X_{id}^a$ are the state variables deviation of the i^{th} USV,

Corresponding Author: Zaopeng Dong, E-mail: dongzaopeng@whut.edu.cn

$\tilde{U}_i^a = U_i^a - U_{id}^a$ are the input variables deviation of the i^{th} USV, A_a and B_a are the Jacobi matrices shown below:

$$A_a = \left.\frac{\partial f}{\partial X_i^a}\right|_{\substack{X_i^a = X_{id}^a \\ U_i^a = U_{id}^a}}, \quad B_a = \left.\frac{\partial f}{\partial U_i^a}\right|_{\substack{X_i^a = X_{id}^a \\ U_i^a = U_{id}^a}}$$

Step 3: Model Discretization

To facilitate the numerical analysis, the linearized model (11) of the i^{th} USV is approximately discretized by Euler's method at moment k, then we have:

$$\dot{\tilde{X}}_i^a(k) = \left(\tilde{X}_i^a(k+1) - \tilde{X}_i^a(k)\right)/h \tag{12}$$

Bringing equation (12) into the equation (11), the equation after linear discretization of the nonlinear system of the i^{th} USV at any of the desired trajectory reference points $\left(X_{id}^a, U_{id}^a\right)$ can be obtained as:

$$\begin{aligned} \tilde{X}_i^a(k+1) &= \dot{\tilde{X}}_i^a(k)\cdot h + \tilde{X}_i^a(k) \\ &= \left(A_a \cdot h + I\right)\cdot \tilde{X}_i^a(k) + B_a \cdot h \cdot \tilde{U}_i^a(k) \\ &= A_k \tilde{X}_i^a(k) + B_k \tilde{U}_i^a(k) \end{aligned} \tag{13}$$

Where $A_k = A_a \cdot h + I$, $B_k = B_a \cdot h$.

To prepare for the subsequent analysis, we combine the state variable deviation $\tilde{X}_i^a(k)$ with the input variable deviation $\tilde{U}_i^a(k-1)$ of the i^{th} USV and a new extended system state variable $\xi_i^a(k) = \left[\tilde{X}_i^a(k) \quad \tilde{U}_i^a(k-1)\right]^T$ is redefined.

Bringing the variable $\xi_i^a(k)$ into equation (13), a new system state space model of the i^{th} USV can be obtained as follows:

$$\begin{cases} \xi_i^a(k+1) = \tilde{A}_k \xi_i^a(k) + \tilde{B}_k \Delta U_i^a(k) \\ \tilde{X}_i^a(k) = \tilde{C}_k \xi_i^a(k) \end{cases} \tag{14}$$

Corresponding Author: Zaopeng Dong, E-mail: dongzaopeng@whut.edu.cn

Where $\tilde{A}_k = \begin{bmatrix} A_k & B_k \\ 0_{2\times 6} & I_2 \end{bmatrix}$, $\tilde{B}_k = \begin{bmatrix} B_k \\ I_2 \end{bmatrix}$, $\Delta U_i^a(k) = \tilde{U}_i^a(k) - \tilde{U}_i^a(k-1)$.

If $a=0$, $\tilde{C}_k = [I_4 \quad 0_{4*2}]$, if $a=1$, $\tilde{C}_k = [I_6 \quad 0_{6*2}]$.

To simplify the calculation, in the predictive horizon N_p, it is assumed that:

$$\begin{aligned} &\tilde{A}_{k+m} = \tilde{A}_k, \tilde{B}_{k+m} = \tilde{B}_k, m = 1,2,\cdots,N_p - 1 \\ &U_{id}^a(k+m) = U_{id}^a(k), m = 1,2,\cdots,N_c - 1 \end{aligned} \tag{15}$$

Thus, we can obtain:

$$\Delta U_i^a(k) = U_i^a(k) - U_i^a(k-1) \tag{16}$$

Combining equations (14), (15) and (16), the predicted output expression of the system is given as:

$$\Gamma_i^a(k) = \psi_k \xi_i^a(k) + \Theta_k \Delta\Phi_i^a(k) \tag{17}$$

Where $\Gamma_i^a(k) = \begin{bmatrix} \tilde{X}_i^a(k+1) \\ \tilde{X}_i^a(k+2) \\ \vdots \\ \tilde{X}_i^a(k+N_p) \end{bmatrix}$, $\psi_k = \begin{bmatrix} \tilde{C}_k\tilde{A}_k \\ \tilde{C}_k\tilde{A}_k^2 \\ \vdots \\ \tilde{C}_k\tilde{A}_k^{N_p} \end{bmatrix}$, $\Delta\Phi_i^a(k) = \begin{bmatrix} \Delta U_i^a(k) \\ \Delta U_i^a(k+1) \\ \vdots \\ \Delta U_i^a(k+N_c-1) \end{bmatrix}$,

$$\Theta_k = \begin{bmatrix} \tilde{C}_k\tilde{B}_k & 0 & 0 & 0 \\ \tilde{C}_k\tilde{A}_k\tilde{B}_k & \tilde{C}_k\tilde{B}_k & 0 & 0 \\ \vdots & \vdots & \ddots & \vdots \\ \tilde{C}_k\tilde{A}_k^{N_c-1}\tilde{B}_k & \tilde{C}_k\tilde{A}_k^{N_c-2}\tilde{B}_k & \cdots & \tilde{C}_k\tilde{B}_k \\ \tilde{C}_k\tilde{A}_k^{N_c}\tilde{B}_k & \tilde{C}_k\tilde{A}_k^{N_c-1}\tilde{B}_k & \cdots & \tilde{C}_k\tilde{A}_k\tilde{B}_k \\ \vdots & \vdots & \ddots & \vdots \\ \tilde{C}_k\tilde{A}_k^{N_p-1}\tilde{B}_k & \tilde{C}_k\tilde{A}_k^{N_p-2}\tilde{B}_k & \cdots & \tilde{C}_k\tilde{A}_k^{N_p-N_c}\tilde{B}_k \end{bmatrix}.$$

Step 4: Optimization problems

According to the actual requirements of trajectory tracking, the cost function can be designed as below:

$$J_i^a(k) = \sum_{i=0}^{N_c-1} \left\| \tilde{X}_i^a(k+i) \right\|_Q^2 + \sum_{i=0}^{N_c-1} \left\| \Delta U_i^a(k+i) \right\|_R^2 + \tilde{X}_i^a(k+N_c)^T P \tilde{X}_i^a(k+N_c) \tag{18}$$

Corresponding Author: Zaopeng Dong, E-mail: dongzaopeng@whut.edu.cn

The first of these terms reflects the system's ability to track the desired trajectory, and the second reflects the system's requirement for smooth changes in control variables. Q and R are weighting matrices, and the function of the first two expressions is to enable the system to track up the desired trajectory as quickly and smoothly as possible. The third term is a terminal penalty function that converges the terminal state of the system in the terminal domain Ω ($\exists\alpha\in(0,\infty)$ $\Omega=\left\{\tilde{X}_i^a(k)\in\bar{X}_i^a\middle|\tilde{X}_i^a(k)^T P\tilde{X}_i^a(k)\le\alpha\right\}$). This term is crucial for stability analysis, but can be omitted in general when used in practice. In addition, in the actual control process, some constraints on the state quantities as well as the control quantities of the system need to be satisfied, generally as follows.

$$\begin{cases}\Delta U_{\min}\le\Delta U_i^a(k+j)\le\Delta U_{\max} & j=0,1,2,\cdots N_c-1\\ U_{\min}\le U_i^a(k+j)\le U_{\max} & j=0,1,2,\cdots N_c-1\\ \tilde{X}_{i\min}^a\le\tilde{X}_i^a(k+j)\le\tilde{X}_{i\max}^a & j=0,1,2,\cdots N_c-1\end{cases}\tag{19}$$

Where $\bar{X}_i^a$ is the set of output variables constraints, $\Delta U_{\min}$ and $\Delta U_{\max}$ are the control increment constraint extremes, $U_{\min}$ and $U_{\max}$ are the control variable constraint extremes, $\tilde{X}_{i\min}^a$ and $\tilde{X}_{i\max}^a$ are the output variable constraint extremes.

Step 5: Adaptive weights design

In order to improve the control stability as well as the tracking accuracy of MPC, adaptive parameter expressions are designed for the control parameter weighting matrix Q as follows:

$$f(\theta)=\frac{1}{1+e^{-\left|\frac{1}{\theta-\theta_d}\right|}}\tag{20}$$

Where θ represents the current status variable of the USV, θ_d represents the

Corresponding Author: Zaopeng Dong, E-mail: dongzaopeng@whut.edu.cn

desired status variable of the USV.

The expression of the weighting matrix Q for the controller is shown below:

$$Q = diag\left(\left[\frac{1}{1+e^{-\left|\frac{1}{x_i - x_{id}}\right|}} \quad \frac{1}{1+e^{-\left|\frac{1}{y_i - y_{id}}\right|}} \quad \frac{1}{1+e^{-\left|\frac{\pi}{180*(\varphi_i - \varphi_{id})}\right|}} \quad \frac{1}{1+e^{-\left|\frac{1}{u_i - u_{id}}\right|}} \quad \frac{1}{1+e^{-\left|\frac{1}{v_i - v_{id}}\right|}} \quad \frac{1}{1+e^{-\left|\frac{\pi}{180*(r_i - r_{id})}\right|}}\right]\right)$$

In summary, the linear adaptive MPC-based USV tracking control problem is transformed into the problem of solving the minimum of the cost function $J_i^a(k)$ under various constraints. In the next section, the cost function will be transformed into a quadratic programming problem to find a better solution.

3.2. Interior point method for solving quadratic programming

Combining equations (17) and (18), a quadratic equation with respect to $\Delta\Phi_i^a(k)$ can be derived. $\Delta\Phi_i^a(k)$ needs to be designed so that the quadratic equation has a minimum value. Therefore, removing the terms unrelated to $\Delta\Phi_i^a(k)$ will not affect the result, and after simplification the following standard quadratic cost function can be obtained.

$$J\left(\Delta\Phi_i^a(k)\right) = \frac{1}{2}\Delta\Phi_i^a(k)^T H_k \Delta\Phi_i^a(k) + G_k^T \Delta\Phi_i^a(k) \tag{21}$$

Where $H_k = 2\left(\Theta_k{}^T Q' \Theta_k + R\right)$, $G_k = 2\Theta_k{}^T Q'\left[\psi_k \xi_i^a(k)\right]$, $Q' = diag(Q, P)$.

In the USV trajectory tracking process, there is no hard constraint on the deviation of state variables. So the tracking control problem of the USV (virtual USV) can be described as the problem of quadratic programming optimal values as follows:

Corresponding Author: Zaopeng Dong, E-mail: dongzaopeng@whut.edu.cn

$$\arg\min\left\{J\left(\Delta\Phi_i^a\left(k\right)\right)\right\}$$

s.t.

$$I_{N_c}\otimes\left[\Delta u_{iv}^{\min}\quad \Delta r_{iv}^{\min}\right]^T\le\Delta\Phi_i^0\left(k\right)\le I_{N_c}\otimes\left[\Delta u_{iv}^{\max}\quad \Delta r_{iv}^{\max}\right]^T$$

$$I_{N_c}\otimes\left[u_{iv}^{\min}\quad r_{iv}^{\min}\right]^T\le M\Delta\Phi_i^0\left(k\right)+I_{N_c}\otimes U_i^v\left(k-1\right)\le I_{N_c}\otimes\left[u_{iv}^{\max}\quad r_{iv}^{\max}\right]^T$$

$$I_{N_c}\otimes\left[\Delta\tau_{ui}^{\min}\quad \Delta\tau_{ri}^{\min}\right]^T\le\Delta\Phi_i^1\left(k\right)\le I_{N_c}\otimes\left[\Delta\tau_{ui}^{\max}\quad \Delta\tau_{ri}^{\max}\right]^T$$

$$I_{N_c}\otimes\left[\tau_{ui}^{\min}\quad \tau_{ri}^{\min}\right]^T\le M\Delta\Phi_i^1\left(k\right)+I_{N_c}\otimes U_i\left(k-1\right)\le I_{N_c}\otimes\left[\tau_{ui}^{\max}\quad \tau_{ri}^{\max}\right]^T$$

Where $M=\begin{bmatrix}1&0&\cdots&0\\1&1&0&\vdots\\\vdots&\vdots&\ddots&0\\1&1&\cdots&1\end{bmatrix}_{N_c\times N_c}\otimes I_2$

For a standard quadratic cost function like equation (21), this is the same form of problem description for USV and virtual USV, so next we take the actual USV as an example, and the inequality constraint model can be converted to the following form:

$$\begin{aligned}&\min f\left(\Delta\Phi_i\left(k\right)\right)\\&\textit{s.t.}\\&I_{2N_c}\cdot\Delta\Phi_i\left(k\right)\le I_{N_c}\otimes\left[\Delta\tau_{ui}^{\max}\quad \Delta\tau_{ri}^{\max}\right]^T\\&-I_{2N_c}\cdot\Delta\Phi_i\left(k\right)\le -I_{N_c}\otimes\left[\Delta\tau_{ui}^{\min}\quad \Delta\tau_{ri}^{\min}\right]^T\\&M\Delta\Phi_i\left(k\right)\le I_{N_c}\otimes\left[\left[\tau_{ui}^{\max}\quad \tau_{ri}^{\max}\right]^T-U_i\left(k-1\right)\right]\\&-M\Delta\Phi_i\left(k\right)\le -I_{N_c}\otimes\left[\left[\tau_{ui}^{\min}\quad \tau_{ri}^{\min}\right]^T+U_i\left(k-1\right)\right]\end{aligned}\tag{22}$$

The Lagrange function of model (22) can be expressed as:

$$L\left(\Delta\Phi_i\left(k\right),\mu\right)=\frac{1}{2}\Delta\Phi_i\left(k\right)^T H_k\Delta\Phi_i\left(k\right)+G_k{}^T\Delta\Phi_i\left(k\right)+\sum_{j=1}^{4}\mu_j\left(h_j^T\chi-t_j\right)\tag{23}$$

Where $h_1=I_{2N_c}$, $h_2=-I_{2N_c}$, $h_3=M^T$, $h_4=-M^T$,

$$t_1=I_{N_c}\otimes\left[\Delta\tau_{ui}^{\max}\quad \Delta\tau_{ri}^{\max}\right]^T, t_2=-I_{N_c}\otimes\left[\Delta\tau_{ui}^{\min}\quad \Delta\tau_{ri}^{\min}\right]^T,$$

$$t_3=I_{N_c}\otimes\left[\left[\tau_{ui}^{\max}\quad \tau_{ri}^{\max}\right]^T-U_i\left(k-1\right)\right],$$

Corresponding Author: Zaopeng Dong, E-mail: dongzaopeng@whut.edu.cn

$$t_4 = -I_{N_c} \otimes \left[\begin{bmatrix} \tau_{ui}^{\min} & \tau_{ri}^{\min} \end{bmatrix}^T + U_i(k-1) \right].$$

In this section, the primal-dual method is used, and the KKT condition after adding a tiny amount of perturbation τ in equation (23) is:

$$\begin{cases} H_k \Delta\Phi_i(k) + G_k + \sum_{j=1}^{4} \mu_j h_j^T = 0 \\ h_j^T \Delta\Phi_i(k) \le t_j \\ \mu_j \left(h_j^T \Delta\Phi_i(k) - t_j \right) = -\tau_j \\ \mu_j \ge 0,\ j = 1,2,3,4 \end{cases} \tag{24}$$

In order to check faster whether the solution is in the constraint space, a relaxation variable s_j is introduced in the system of inequality equations, satisfying $s_j = t_j - h_j^T \Delta\Phi_i(k)$. Equation (24) becomes the following form:

$$\begin{cases} H_k \Delta\Phi_i(k) + G_k + \sum_{j=1}^{4} \mu_j h_j^T = 0 \\ h_j^T \Delta\Phi_i(k) + s_j = t_j \\ \mu_j s_j = \tau_j \\ \mu_j, s_j \ge 0,\ j = 1,2,3,4 \end{cases} \tag{25}$$

Writing equation (25) as a matrix as:

$$F\left(\Delta\Phi_i(k), \mathrm{s}, \mu\right) = \begin{bmatrix} H_k \Delta\Phi_i(k) + G_k + \mu h^T \\ h^T \Delta\Phi_i(k) + s - t \\ \mu s - \tau \end{bmatrix} = 0 \tag{26}$$

Where $\mu = \begin{bmatrix} \mu_1 & \mu_2 & \mu_3 & \mu_4 \end{bmatrix}$, $h^T = \begin{bmatrix} h_1^T & h_2^T & h_3^T & h_4^T \end{bmatrix}^T$, $t = \begin{bmatrix} t_1 & t_2 & t_3 & t_4 \end{bmatrix}^T$, $s = \begin{bmatrix} s_1 & s_2 & s_3 & s_4 \end{bmatrix}^T$, $\tau = \sum_{j=1}^{4} \tau_j$.

Newton's method is used to solve the above system of equations (26), and at moment m we have:

$$F\left(\Delta\Phi_i(k)_m, \mathrm{s}_m, \mu_m\right) + F'\left(\Delta\Phi_i(k)_m, \mathrm{s}_m, \mu_m\right)\left(\Delta\left(\Delta\Phi_i(k)_m\right), \Delta\mathrm{s}_m, \Delta\mu_m\right) = 0 \tag{27}$$

Corresponding Author: Zaopeng Dong, E-mail: dongzaopeng@whut.edu.cn

Equation (27) can be converted to:

$$\begin{bmatrix} H_k & 0 & h^T \\ h^T & I & 0 \\ 0 & \mu_m & s_m^T \end{bmatrix} \begin{bmatrix} \Delta\left(\Delta\Phi_i\left(k\right)_m\right) \\ \Delta \mathrm{s}_m \\ \Delta\mu_m \end{bmatrix} = -\begin{bmatrix} H_k\Delta\Phi_i\left(k\right)_m + G_k + \mu_m h^T \\ h^T\Delta\Phi_i\left(k\right)_m + s_m - t \\ \mu_m s_m - \tau_m \end{bmatrix} \tag{28}$$

The value of $\left(\Delta\left(\Delta\Phi_i\left(k\right)_m\right), \Delta \mathrm{s}_m, \Delta\mu_m\right)$ at moment m can be gotten by equation (28), from which the variables at moment $m+1$ are updated as:

$$\left(\chi_{m+1}, \mathrm{s}_{m+1}, \mu_{m+1}\right) = \left(\chi_m, \mathrm{s}_m, \mu_m\right) + \alpha\left(\Delta\left(\Delta\Phi_i\left(k\right)_m\right), \Delta \mathrm{s}_m, \Delta\mu_m\right) \tag{29}$$

Where α is the step size, and in order to satisfy $s_{j,\mathrm{m}}, \mu_{j,\mathrm{m}} \geq 0$ ($s_{j,\mathrm{m}}, \mu_{j,\mathrm{m}}$ represents s_j, μ_j at the moment of m), define $\alpha_s = \min\left\{1, \min\limits_{\Delta \mathrm{s}_{j,\mathrm{m}}<0}\left\{\dfrac{\mathrm{s}_{j,\mathrm{m}}}{-\Delta \mathrm{s}_{j,\mathrm{m}}}\right\}\right\}$, $\alpha_\mu = \min\left\{1, \min\limits_{\Delta\mu_{j,\mathrm{m}}<0}\left\{\dfrac{\mu_{j,\mathrm{m}}}{-\Delta\mu_{j,\mathrm{m}}}\right\}\right\}$ and take $\alpha = \min\left(\alpha_s, \alpha_\mu\right)$.

Also update τ for moment $m+1$: $\tau_{m+1} = \sigma\sum_{j=1}^{4}\mu_{j,m}s_{j,m}$, $\sigma \in [0,1]$. Repeat the above operation until the solution of the system of equations (26) is obtained, i.e., $\left|f^{m+1} - f^m\right| < \varepsilon$ is satisfied. To ensure the correctness of the solution, the condition that the Newton method of solving the equation stops must be supplemented by $\tau_m \leq \delta$. Where ε and δ are both minimal values, f^{m+1} is the value of $f\left(\Delta\Phi_i\left(k\right)\right)$ at moment $m+1$, and f^m is the value of $f\left(\Delta\Phi_i\left(k\right)\right)$ at moment m.

3.3. Formation desired trajectory smoothing

In the actual tracking process, as the leader has to track a time-related desired trajectory from the stationary state at the initial moment, the head angle and velocity

Corresponding Author: Zaopeng Dong, E-mail: dongzaopeng@whut.edu.cn

are bound to change drastically in the early stage. Thus, the desired trajectory of the follower USV (deduced from the position information of the leader USV at this moment) must also be messy in the early stage, which causes great difficulties to our control. Therefore, in this paper, when generating the desired trajectory of the follower USV, the operation of smooth transition is done for it. It is mainly divided into the following two parts:

1. The track of the virtual USV is used instead of the track of the actual USV in the first phase.

2. The improved discrete tracking-differentiator is designed to smooth the transition of the virtual leader's bow angle, and the desired trajectory smoothing effect is achieved by reducing the rate of change of the bow angle.

The input and output schematic of the discrete tracking-differentiator is shown in Fig.3 below:

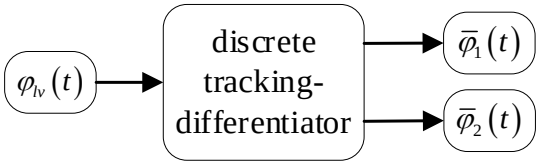

Figure 3. Schematic diagram of discrete tracking-differentiator

Where $\varphi_{lv}(t)$ is the virtual leader's bow angle, after the tracking-differentiator, two output signals $\bar{\varphi}_1(t)$ and $\bar{\varphi}_2(t)$ are obtained, for the virtual leader's bow angle signal $\varphi_{lv}(t)$, the output signal $\bar{\varphi}_1(t)$ tracks $\varphi_{lv}(t)$, $\bar{\varphi}_2(t)$ is the differentiation of $\bar{\varphi}_1(t)$. It can be seen that the tracking-differentiator dynamic system can not only quickly track the virtual leader's bow angle signal, but also extract the approximate

Corresponding Author: Zaopeng Dong, E-mail: dongzaopeng@whut.edu.cn

differentiation signal. In the actual USV control process, the calculation formula of the discrete form of the tracking-differentiator is shown below:

$$\begin{cases} \bar{\varphi}_1(k+1) = \bar{\varphi}_1(k) + h\bar{\varphi}_2(k) \\ \bar{\varphi}_2(k+1) = \bar{\varphi}_2(k) + h\{-\alpha^2[\bar{\varphi}_1(k) - \varphi_v(k)] - 2\alpha\bar{\varphi}_2(k)\} \end{cases} \tag{30}$$

Where h is sampling step and α is artificially designed speed coefficient.

The speed coefficient α in the conventional tracking-differentiator is often a constant, representing how fast or slow the tracking is. If a small value is taken, the smoothed desired path will deviate from the real desired trajectory for a long time, which leads to slow tracking and low accuracy. If a larger value is taken, the tracking is too fast, which will lead to poor smoothing effect, so this section makes some improvements to the speed coefficient by changing it from a constant to a time-varying factor.

The equation for the improved discrete tracking-differentiator is shown below:

$$\begin{cases} \bar{\varphi}_1(k+1) = \bar{\varphi}_1(k) + h\bar{\varphi}_2(k) \\ \bar{\varphi}_2(k+1) = \bar{\varphi}_2(k) + h\{-\alpha^2 k^2[\bar{\varphi}_1(k) - \varphi_v(k)] - 2\alpha k\bar{\varphi}_2(k)\} \end{cases} \tag{31}$$

In summary, the desired position information of the i^{th} follower USV can be converted by equation (5) as:

$$Y_j^d = Y_v + R(\bar{\varphi}_1) \cdot L_j \tag{32}$$

Where $R(\bar{\varphi}_1)$ is the coordinate transformation matrix satisfying $R(\bar{\varphi}_1) = \begin{bmatrix} \cos(\bar{\varphi}_1) & -\sin(\bar{\varphi}_1) \\ \sin(\bar{\varphi}_1) & \cos(\bar{\varphi}_1) \end{bmatrix}$, L_j is the formation of the j^{th} follower USV satisfying $L_j = \begin{bmatrix} L_{xj} & L_{yj} \end{bmatrix}^T$, Y_v is the location of the virtual leader USV satisfying $Y_v = \begin{bmatrix} x_v & y_v \end{bmatrix}^T$.

Corresponding Author: Zaopeng Dong, E-mail: dongzaopeng@whut.edu.cn

3.4. Dual mode switching conditions

Due to the dual MPC controller design, the tracking error of the virtual USV for the desired trajectory will affect the tracking accuracy of the actual USV under the influence of the time-varying desired state variable and external disturbance factors, so we need to set the appropriate judgment conditions so that the controller can be converted from the dual MPC controller to the single MPC control, and the flow chart is shown in Fig.4.

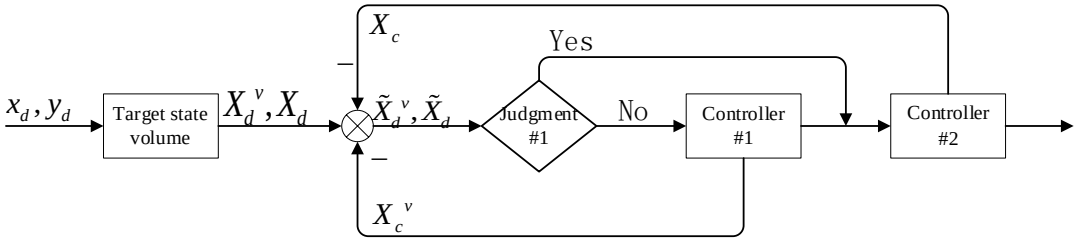

Figure 4. Controller switching flow chart

Judgment #1 is defined as follows.

$$X_{id} = \begin{cases} \begin{bmatrix} x_{iv} & y_{iv} & \varphi_{iv} & u_{id} & v_{id} & r_{id} \end{bmatrix} & , \left\| \tilde{X}_{id}^{\ v} \right\|_2 > \delta \\ \begin{bmatrix} x_{id} & y_{id} & \varphi_{id} & u_{id} & v_{id} & r_{id} \end{bmatrix} & , \left\| \tilde{X}_{id}^{\ v} \right\|_2 < \delta \end{cases} \tag{33}$$

When condition $\left\| \tilde{X}_{id}^{\ v} \right\|_2 < \delta$ is satisfied, only controller #2 is implemented.

For equation (32), the judgment #2 is also introduced as follows.

$$Y_j^d = \begin{cases} Y_v + R(\bar{\varphi}_1) \cdot L_j & , \left\| X_l - X_l^{\ v} \right\|_2 > \varepsilon \\ Y + R(\varphi_l) \cdot L_j & , \left\| X_l - X_l^{\ v} \right\|_2 < \varepsilon \end{cases} \tag{34}$$

Where δ, ε are small values.

3.5. Nonlinear disturbances observer

In the actual marine environment, USVs are often affected by external

Corresponding Author: Zaopeng Dong, E-mail: dongzaopeng@whut.edu.cn

disturbances, and the robustness of MPC can't be completely offset in the face of larger disturbances. Therefore, in this section, a nonlinear state observer is designed to observe and compensate the disturbances in the longitudinal and corner directions to further improve the anti-interference capability of the controller.

The mathematical model expression for the motion of the i^{th} USV under the consideration of disturbance is as follows:

$$\begin{cases} \dot{\boldsymbol{\eta}}_i = \boldsymbol{R}(\varphi_i)\boldsymbol{v}_i \\ \dot{\boldsymbol{v}}_i = \boldsymbol{M}_i^{-1}\left(-\boldsymbol{C}(\boldsymbol{v}_i)\boldsymbol{v}_i - \boldsymbol{D}_i\boldsymbol{v}_i + \boldsymbol{\tau}_i + \boldsymbol{w}_i\right) \end{cases} \tag{35}$$

Define $d_{1i} = \omega_{ui} / m_{1i}$, $d_{2i} = \omega_{vi} / m_{2i}$, $d_{3i} = \omega_{ri} / m_{3i}$, $d_i = \begin{bmatrix} d_{1i} & d_{2i} & d_{3i} \end{bmatrix}^T$. The following disturbance observer equation is established for real-time observation of disturbances.

$$\begin{cases} \hat{d}_i = z_i + L \cdot \boldsymbol{v}_i \\ \dot{z}_i = -L\hat{d}_i - L \cdot \boldsymbol{M}_i^{-1}\left(-\boldsymbol{C}(\boldsymbol{v}_i)\boldsymbol{v}_i - \boldsymbol{D}_i\boldsymbol{v}_i + \boldsymbol{\tau}_i\right) \end{cases} \tag{36}$$

Where $\hat{d}_i$ is the disturbance estimate; z_i is a constructive variable; L is the disturbance observer bandwidth and is positive.

Combined with the nonlinear observer design (36), the mathematical model (35) can be extended as:

$$\begin{cases} \dot{\boldsymbol{\eta}}_i = \boldsymbol{R}(\varphi_i)\boldsymbol{v}_i \\ \dot{\boldsymbol{v}}_i = \boldsymbol{M}_i^{-1}\left(-\boldsymbol{C}(\boldsymbol{v}_i)\boldsymbol{v}_i - \boldsymbol{D}_i\boldsymbol{v}_i + \boldsymbol{\tau}_i\right) + d_i \\ \dot{z}_i = -L\hat{d}_i - L \cdot \boldsymbol{M}_i^{-1}\left(-\boldsymbol{C}(\boldsymbol{v}_i)\boldsymbol{v}_i - \boldsymbol{D}_i\boldsymbol{v}_i + \boldsymbol{\tau}_i\right) \end{cases} \tag{37}$$

The Runge-Kutta method is used to update the equation (37) to find the next moment of x_i, y_i, φ_i, u_i, v_i, r_i, z. These values are substituted back into equation (37) and updated for $\hat{d}$.

Corresponding Author: Zaopeng Dong, E-mail: dongzaopeng@whut.edu.cn

$$\hat{d}_i = z_i + L \cdot \boldsymbol{v}_i \tag{38}$$

Therefore, the control law for the cooperative formation trajectory tracking control of the i^{th} USV can be expressed in the following form.

$$U_i(k) = U_i(k-1) + \Delta U_i(k) + \boldsymbol{M}_i^{-1} \hat{\mathrm{d}}_i(k) \tag{39}$$

Where $\Delta U_i(k)$ is taken as the first term of the better solution $\Delta\Phi_i(k)$ obtained using MPC at the current k moments.

3.6. Collision between individuals

In order to prevent collisions between formations during USVs voyages, a collision avoidance strategy is designed, as shown in Figure 5 below.

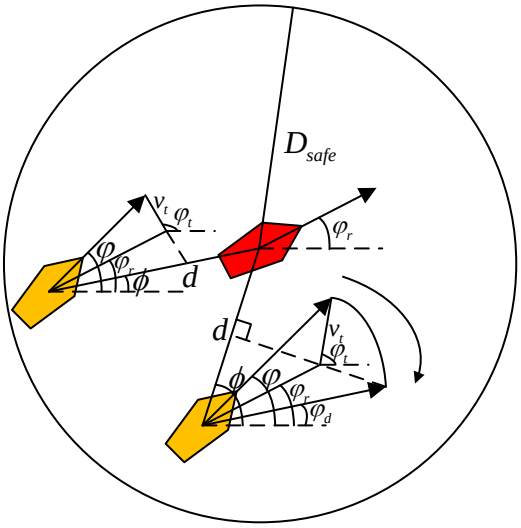

Figure 5. Collision avoidance strategy

When condition $d \le D_{safe}$ is satisfied, the collision avoidance strategy is executed, take $\varphi_{td} = \begin{cases} \phi + \pi/2, \varphi \ge \phi \\ \phi - \pi/2, \varphi < \phi \end{cases}$, $\varphi_t = \begin{cases} \varphi_{td}, |\varphi_t - \phi| \le \pi/2 \\ \varphi_t, |\varphi_t - \phi| > \pi/2 \end{cases}$.

Where d is the distance between the two USVs, D_{safe} is the safe distance used to determine whether to perform collision avoidance, ϕ is the angle between the two

Corresponding Author: Zaopeng Dong, E-mail: dongzaopeng@whut.edu.cn

USVs positions, v_t is the speed of the follower relative to the leader, φ_r is the heading angle of the leader, φ_t is the angle of the relative speed v_t. When $|\varphi_t - \phi| \le \pi/2$, according to The Law of Sines, desired angle φ_d needs to satisfy $\frac{|v|}{\sin(\varphi_r - \varphi_{td})} = \frac{|v_r|}{\sin(\varphi_d - \varphi_{td})}$, otherwise φ_d doesn't change. Where $|v|$ is the speed size of the follower and $|v_r|$ is the speed size of the leader.

4. Stability analysis

4.1. Stability of nonlinear observer

Define $\tilde{d}_i = \hat{d}_i - d_i$ and let the Lyapunov equation be $V = 1/2 \cdot \tilde{d}_i^2$. Derivative for the Lyapunov function.

$$\begin{aligned} \dot{V} &= \tilde{d}_i \cdot \dot{\tilde{d}}_i = \tilde{d}_i \left(\dot{\hat{d}}_i - \dot{d}_i \right) = \tilde{d}_i \left(\dot{z}_i + L \cdot \dot{\boldsymbol{v}}_i - \dot{d}_i \right) \\ &= \tilde{d}_i \left(-L\hat{d}_i - L \cdot \boldsymbol{M}_i^{-1} \left(-\boldsymbol{C}(\boldsymbol{v}_i)\boldsymbol{v}_i - \boldsymbol{D}_i\boldsymbol{v}_i + \boldsymbol{\tau}_i \right) + L \cdot \dot{\boldsymbol{v}}_i - \dot{d}_i \right) \\ &= \tilde{d}_i \left(-L\left(\hat{d}_i - d_i \right) - L \cdot \boldsymbol{M}_i^{-1} \left(-\boldsymbol{M}_i\dot{\boldsymbol{v}}_i - \boldsymbol{C}(\boldsymbol{v}_i)\boldsymbol{v}_i - \boldsymbol{D}_i\boldsymbol{v}_i + \boldsymbol{\tau}_i + \boldsymbol{w}_i \right) - \dot{d}_i \right) \end{aligned} \tag{40}$$

Combining with equation (2), the above equation can be rectified to obtain $\dot{V} = -L\tilde{d}^2 - \dot{d}\tilde{d}$, When $\dot{d}$ is bounded, $\tilde{d}$ converges. From the stability proof, it can be concluded that the designed nonlinear observer can accurately observe the magnitude of the disturbance. Since the USV's actuator is underdriven, only additional compensation can be made for longitudinal and bow angular velocities, and lateral disturbances will be resisted by the robustness of the MPC, the feasibility of which will be verified by simulation later.

4.2. Stability of the MPC

For the controlled model shown as equation (14), it is assumed that the optimal

Corresponding Author: Zaopeng Dong, E-mail: dongzaopeng@whut.edu.cn

value $\Delta\Phi_i^{a0}(k)$ exists at moment k. The optimal value of the objective function of the optimization proposition at this time (i.e., $J^0(k)$) is taken as the Lyapunov function. From the form of the objective function, $J^0(k) \geq 0$, it is now sufficient to prove that $J^0(k+1) \leq J^0(k)$, stability can be proved.

Where the control sequence is:

$$\Delta\Phi_i^{a0}(k) = \left\{\Delta U_i^{a0}(k|k), \Delta U_i^{a0}(k+1|k), \cdots, \Delta U_i^{a0}(k+N-1|k)\right\}$$

And the sequence of state trajectories at this point is:

$$\Gamma_i^{a0}(k) = \left\{\tilde{X}_i^{a0}(k|k), \tilde{X}_i^{a0}(k+1|k), \cdots, \tilde{X}_i^{a0}(k+N|k)\right\}$$

At the moment $k+1$, define ΔU_f as the last control variable of the complementary control sequence and ΔU_f satisfies the control constraint. The control sequence at this time is a set of feasible solutions for:

$$\Delta\tilde{\Phi}_i^{a}(k) = \left\{\Delta U_i^{a0}(k+1|k), \cdots, \Delta U_i^{a0}(k+N-1|k), \Delta U_f\right\}$$

The corresponding sequence of state trajectories is:

$$\Gamma_i^{a}(k) = \left\{\tilde{X}_i^{a0}(k+1|k), \cdots, \tilde{X}_i^{a0}(k+N|k), f\left(\tilde{X}_i^{a0}(k+N|k), \Delta U_f\right)\right\}$$

Therefore, the following cost function for the feasible solution at $k+1$ moments can be obtained.

$$\begin{aligned} J(k+1) &= J^0(k) - \ell\left(\tilde{X}_i^{a0}(k|k), \Delta U_i^{a0}(k|k)\right) - F\left(\tilde{X}_i^{a0}(k+N|k)\right) \\ &+ \ell\left(f\left(\tilde{X}_i^{a0}(k+N|k), \Delta U_f\right), \Delta U_f\right) + F\left(f\left(\tilde{X}_i^{a0}(k+N|k), \Delta U_f\right)\right) \end{aligned}$$

Define the function $\ell(x,u) = x^T Q x + u^T R u$, $F(x) = x^T P x$.

If MPC has an optimal solution at moment $k+1$, then $J^0(k+1) \leq J(k+1)$. It is sufficient to satisfy the following inequality (41):

Corresponding Author: Zaopeng Dong, E-mail: dongzaopeng@whut.edu.cn

$$\ell\left(f\left(\tilde{X}_i^{a0}\left(k+N|k\right),\Delta U_f\right),\Delta U_f\right)+F\left(f\left(\tilde{X}_i^{a0}\left(k+N|k\right),\Delta U_f\right)\right)-F\left(\tilde{X}_i^{a0}\left(k+N|k\right)\right)\le 0$$

To satisfy

$$J^0\left(k+1\right)\le J\left(k+1\right)\le J^0\left(k\right)-\ell\left(\tilde{X}_i^{a0}\left(k|k\right),\Delta U_i^{a0}\left(k|k\right)\right) \tag{42}$$

The linear state feedback controller is designed as follows,

$$\Delta U_i^a\left(k\right)=K\xi_i^a\left(k\right) \tag{43}$$

Bringing equation (36) into the controlled model (33), can be obtained:

$$\begin{cases}\xi_i^a\left(k+1\right)=\left(\tilde{A}_k+\tilde{B}_kK\right)\xi_i^a\left(k\right)\\ \tilde{X}_i^a\left(k\right)=\tilde{C}_k\xi_i^a\left(k\right)\end{cases} \tag{44}$$

Define $A_N=\tilde{A}_k+\tilde{B}_kK$, A_N is asymptotically stable in the case that the controlled model (40) can be stabilized. Choose

$$\Delta U_f=K\xi_i^a\left(k+N\right) \tag{45}$$

Bringing equation (45) into inequality (41):

$$\xi_i^{aT}\left(k+N\right)\left(A_N{}^T\tilde{C}_k{}^TP\tilde{C}_kA_N-\tilde{C}_k{}^TP\tilde{C}_k+\tilde{C}_k{}^TQ\tilde{C}_k+K^TRK\right)\xi_i^a\left(k+N\right)\le 0 \tag{46}$$

Define $\hat{P}=\tilde{C}_k{}^TP\tilde{C}_k$, $Q_{\text{bar}}=\tilde{C}_k{}^TQ\tilde{C}_k+K^TRK$ and let $\hat{P}$ meets

$$A_N^T\hat{P}A_N-\hat{P}+\kappa Q_{\text{bar}}=0 \tag{47}$$

Where $\kappa>1$.

Since A_N is asymptotically stable and Q_{bar} is a given positive definite symmetric matrix, there exists a unique positive definite symmetric solution to equation (47). Bringing equation (47) back to equation (46), and the following inequality is always true.

$$\left(1-\kappa\right)\xi_i^{aT}\left(k+N\right)\left(\tilde{C}_k{}^TQ\tilde{C}_k+K^TRK\right)\xi_i^a\left(k+N\right)\le 0 \tag{48}$$

Since $\tilde{C}_k$ is a transpose matrix, $\tilde{C}_k{}^{-1}=\tilde{C}_k{}^T$ holds, which is $P=\tilde{C}_k\hat{P}\tilde{C}_k{}^T$.

Corresponding Author: Zaopeng Dong, E-mail: dongzaopeng@whut.edu.cn

From the characteristics of the objective function, it follows that for any $k \geq 0$, there is $J_i^0(k) \geq 0$. It also follows from equation (41), that $J_i^0(k)$ is monotonically decreasing and that $J_i^0(k)$ has a minimum value at $\tilde{X}_i^a(k) = 0$, $\Delta U_i^a(k) = 0$.

Therefore, at time $t \to \infty$, there are $\tilde{X}_i^v(k) = 0, (x_v = x_d, y_v = y_d, \varphi_v = \varphi_d)$ and $\tilde{X}_i(k) = 0, (x_i = x_v, y_i = y_v, \varphi_i = \varphi_v, u_i = u_d, v_i = v_d, r_i = r_d)$.

In summary, it can be demonstrated that the designed MPC controller finally tends to be stable at $t \to \infty$ with $x_i = x_d, y_i = y_d, \varphi_i = \varphi_d, u_i = u_d, v_i = v_d, r_i = r_d$.

5. Simulation results

In this section, the simulation results of the cooperative formation control of USVs will be provided, which highlight the advantages of the proposed improved LMPC method.

5.1. Parameter selection

(1) Model parameter

For the state space equation described by equation (2), the system matrix is: $M_i = diag(25.8, 33.8, 2.76)$, $D_i = diag(12, 17, 0.5)$,

$$\boldsymbol{w}_i = \begin{bmatrix} w_{ui} & w_{vi} & w_{ri} \end{bmatrix}^T = \begin{bmatrix} 10\sin(0.1t) - 5 & \sin(0.1t) & 5\sin(0.1t) + 2 \end{bmatrix}^T$$

(2) Constraint parameter selection

MPC can consider the constraint directly when solving the cost function, and the system constraints during USV motion control are defined as follows:

1. Input variable constraint: $\begin{bmatrix} 0 & -40 \end{bmatrix}^T \leq \tau \leq \begin{bmatrix} 80 & 40 \end{bmatrix}^T$

2. Input Incremental Constraints: $\begin{bmatrix} -20 & -20 \end{bmatrix}^T \leq \Delta\tau \leq \begin{bmatrix} 20 & 20 \end{bmatrix}^T$

Corresponding Author: Zaopeng Dong, E-mail: dongzaopeng@whut.edu.cn

(3) Disturbance observer parameter selection

Set the bandwidth as $L = diag(6,2,6)$

5.2. Coordinated trajectory tracking of three USV formations

Three desired trajectories are used to test the cooperative formation control of three USVs. Firstly, the effectiveness of the proposed control method is compared and verified by setting up a simulation experiment in Case I. Then, the effectiveness of the control method under different cases is verified by setting Case II and Case III, and only the trajectory tracking effect is given due to the limitation of space.

Case I: sinusoidal trajectory tracking

The expression of the desired trajectory: $x_R = t, y_R = 20 \cdot \sin(0.05t)$.

The initial condition of the leader is $x_l = [-4 \quad -4 \quad 0 \quad 0 \quad 0 \quad 0]$. The initial condition of the first follower is $x_1 = [-12 \quad -12 \quad 0 \quad 0 \quad 0 \quad 0]$, whose formation is $L_1 = [-5 \quad -5]$. The initial condition of the second follower is $x_2 = [-13 \quad -2 \quad 0 \quad 0 \quad 0 \quad 0]$, whose formation is $L_2 = [-5 \quad 5]$. The prediction horizon is $N_p = 20$; the control horizon is $N_c = 16$; the sampling period is $T = 0.2s$. The weighting matrices of Virtual USVs are chosen as $Q = I_4$, $R = I_2$ and $\kappa = 8$. The USVs with parameters Q and R using adaptive methods and $\kappa = 1.5$.

Corresponding Author: Zaopeng Dong, E-mail: dongzaopeng@whut.edu.cn

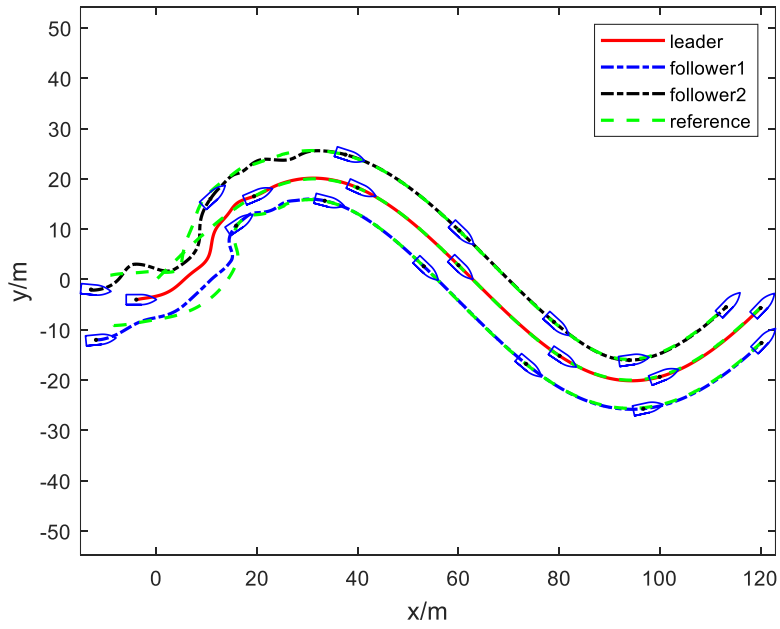

Figure 6. USVs trajectory with IMPC(Case I)

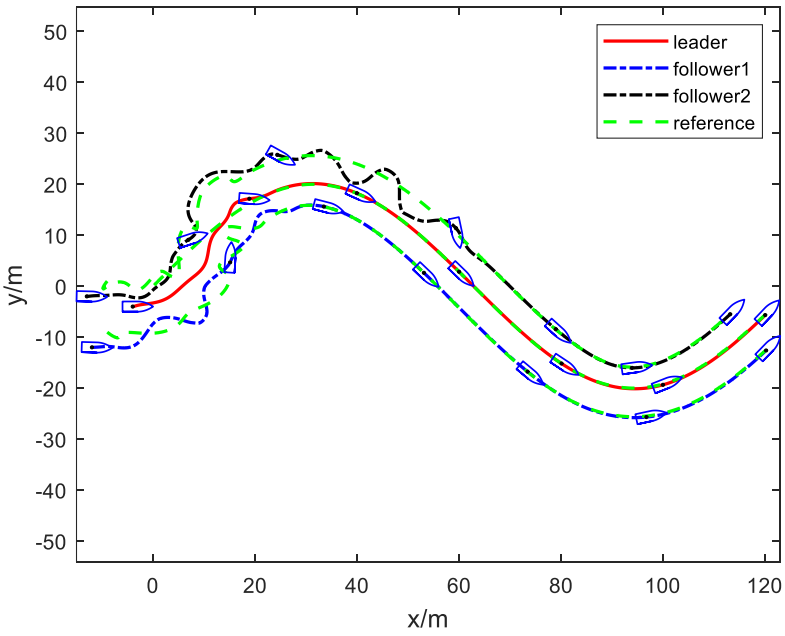

Figure 7. USVs trajectory without smooth(Case I)

Corresponding Author: Zaopeng Dong, E-mail: dongzaopeng@whut.edu.cn

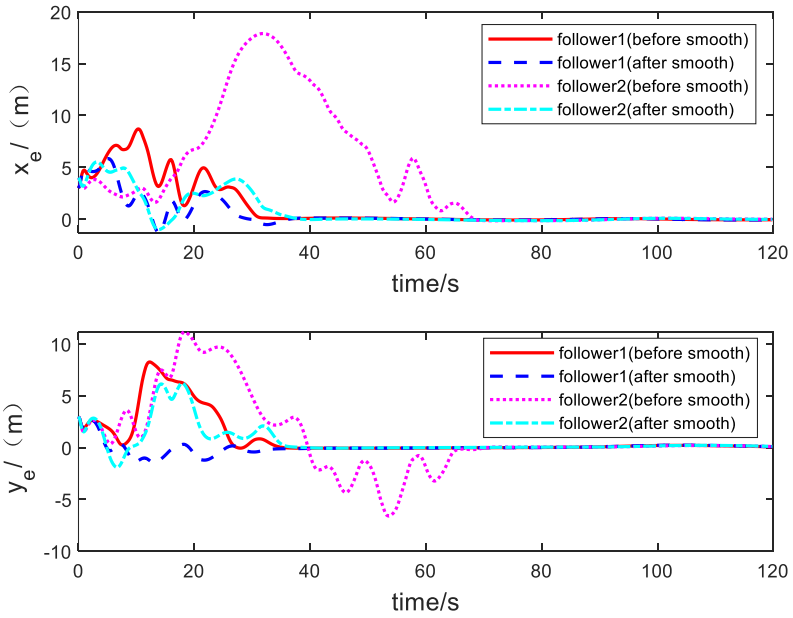

Figure 8. USVs tracking error(Case I)

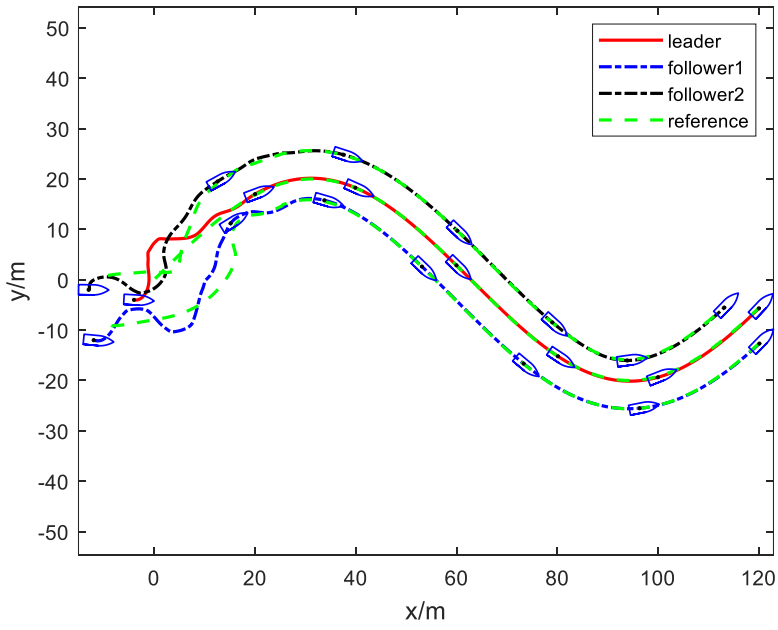

Figure 9. USVs trajectory with MPC(Case I)

Corresponding Author: Zaopeng Dong, E-mail: dongzaopeng@whut.edu.cn

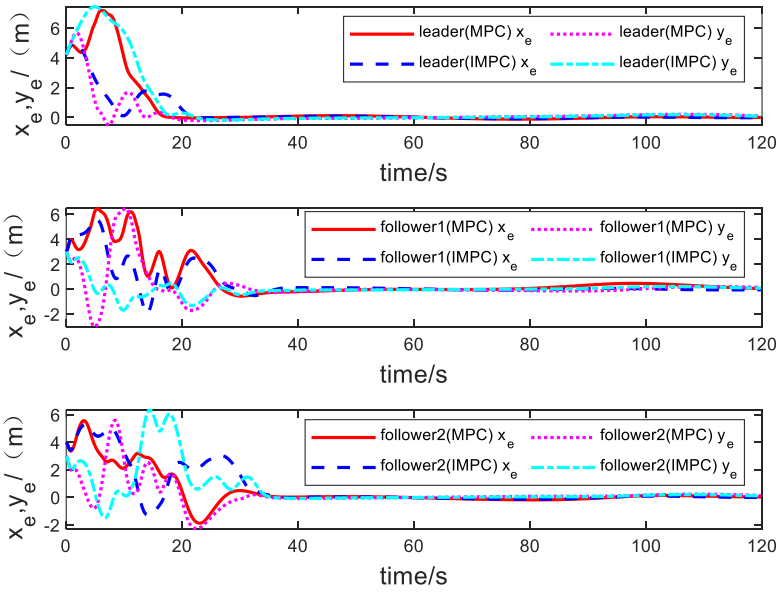

Figure 10. USVs tracking error(Case I)

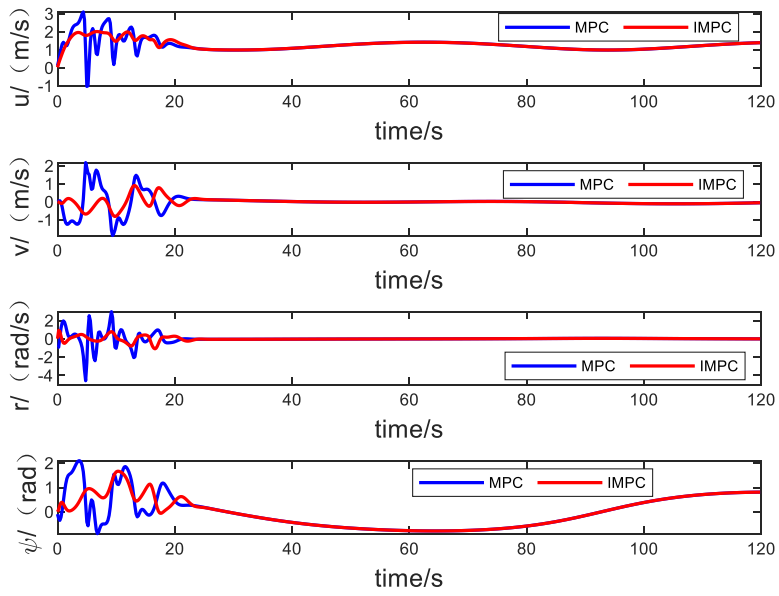

Figure 11. leader status variables(Case I)

Corresponding Author: Zaopeng Dong, E-mail: dongzaopeng@whut.edu.cn

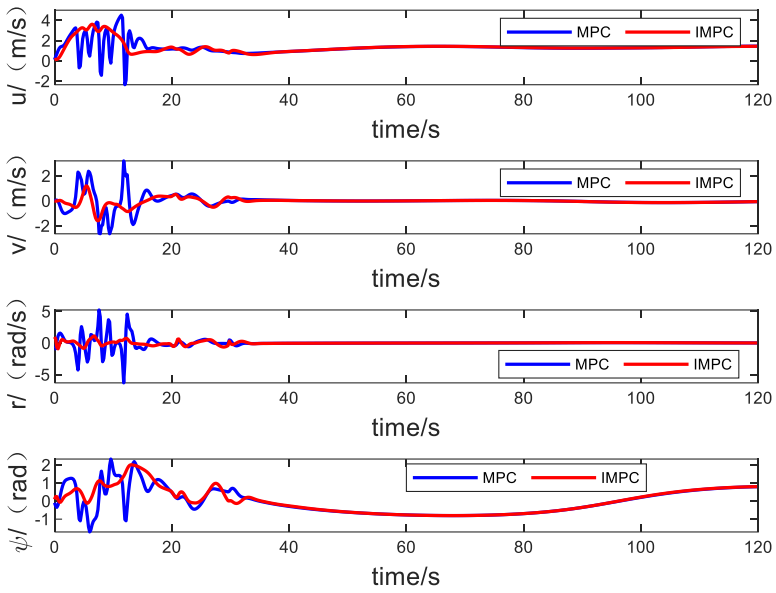

Figure 12. follower 1st status variables(Case I)

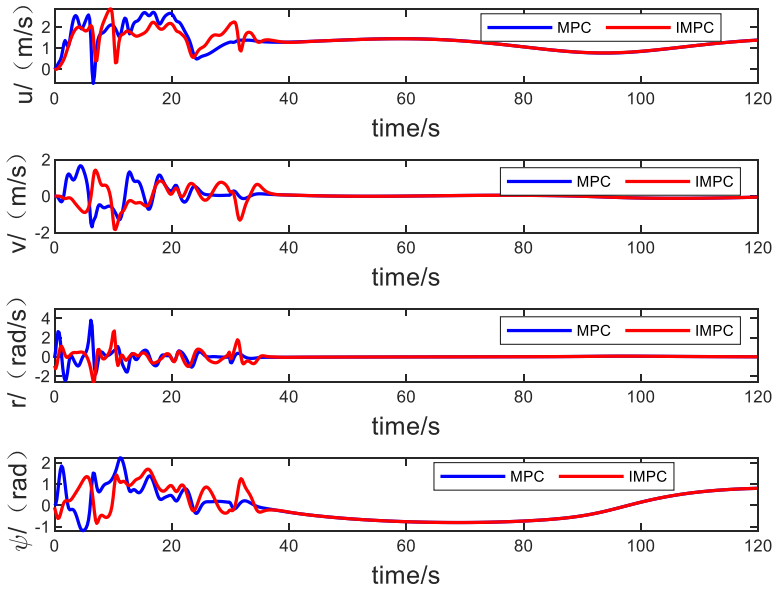

Figure 13. follower 2nd status variables(Case I)

Corresponding Author: Zaopeng Dong, E-mail: dongzaopeng@whut.edu.cn

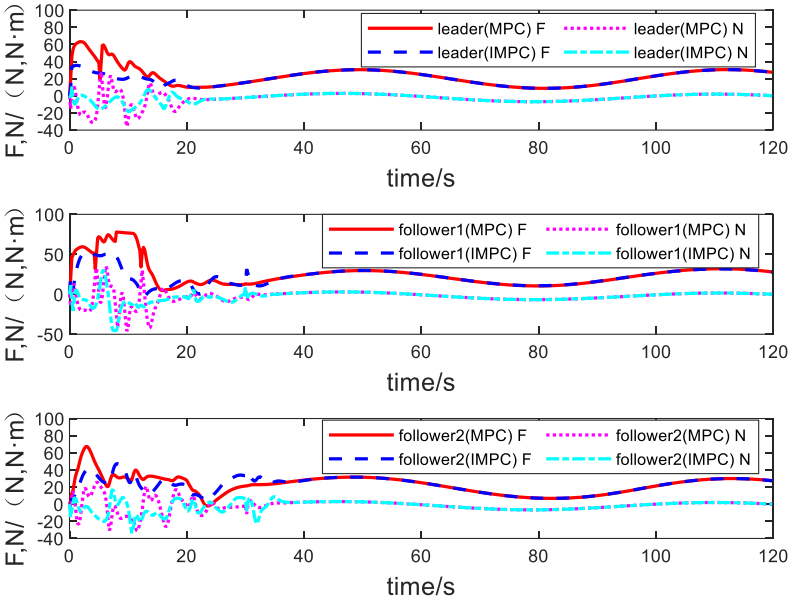

Figure 14. USVs control input signals(Case I)

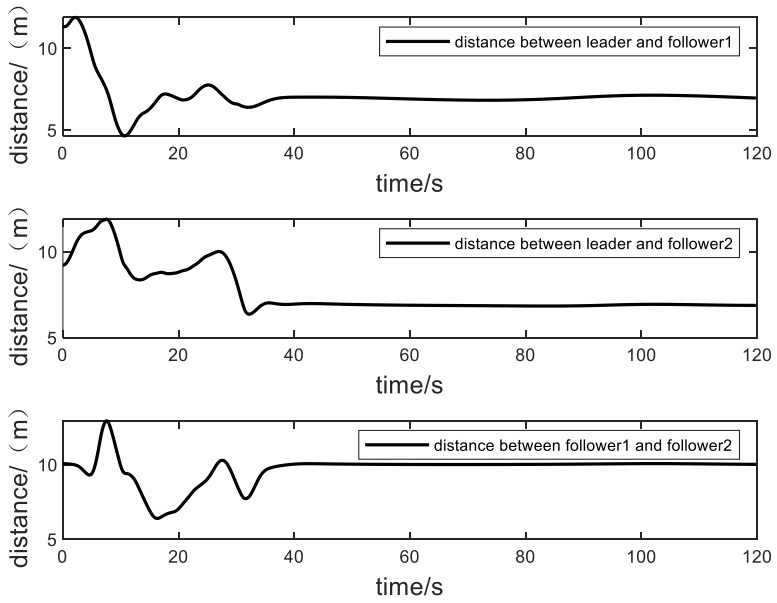

Figure 15.Graph of the change in distance between two USVs(Case I)

Case II: circle-shaped trajectory tracking

The expression of the desired trajectory:

$$x_R = 40 \cdot \sin(0.05t), y_R = 40 - 40 \cdot \cos(0.05t).$$

Corresponding Author: Zaopeng Dong, E-mail: dongzaopeng@whut.edu.cn

The initial condition of the leader is $x_l = [-4 \quad -4 \quad 0 \quad 0 \quad 0 \quad 0]$. The initial condition of the first follower is $x_1 = [-7 \quad -17 \quad 0 \quad 0 \quad 0 \quad 0]$, whose formation is $L_1 = [0 \quad -8]$. The initial condition of the second follower is $x_2 = [-8 \quad 0 \quad 0 \quad 0 \quad 0 \quad 0]$, whose formation is $L_2 = [0 \quad 8]$. The prediction horizon is $N_p = 20$; the control horizon is $N_c = 16$; the sampling period is $T = 0.2s$. The weighting matrices of Virtual USVs are chosen as $Q = I_4$, $R = I_2$ and $\kappa = 1.5$. The USVs with parameters Q and R using adaptive methods and $\kappa = 1.5$.

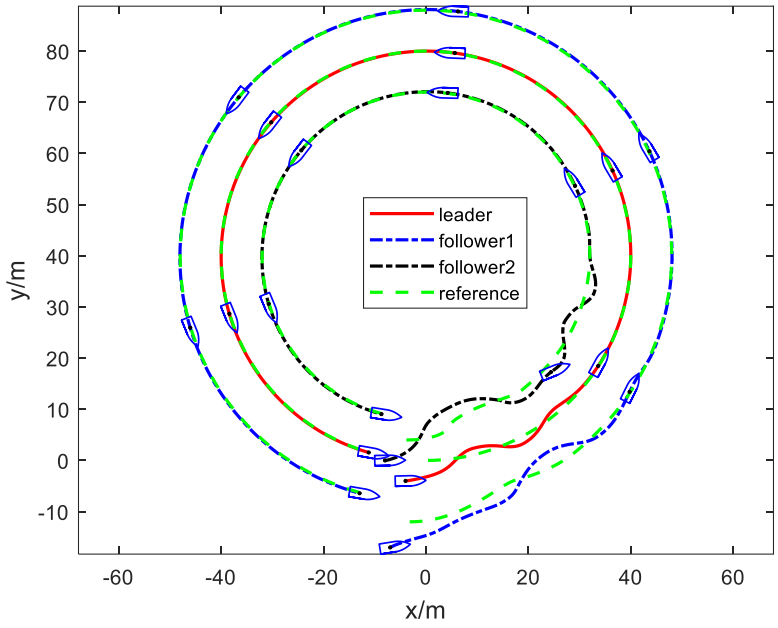

Figure 16. USVs trajectory in xoy plane(Case II)

Corresponding Author: Zaopeng Dong, E-mail: dongzaopeng@whut.edu.cn

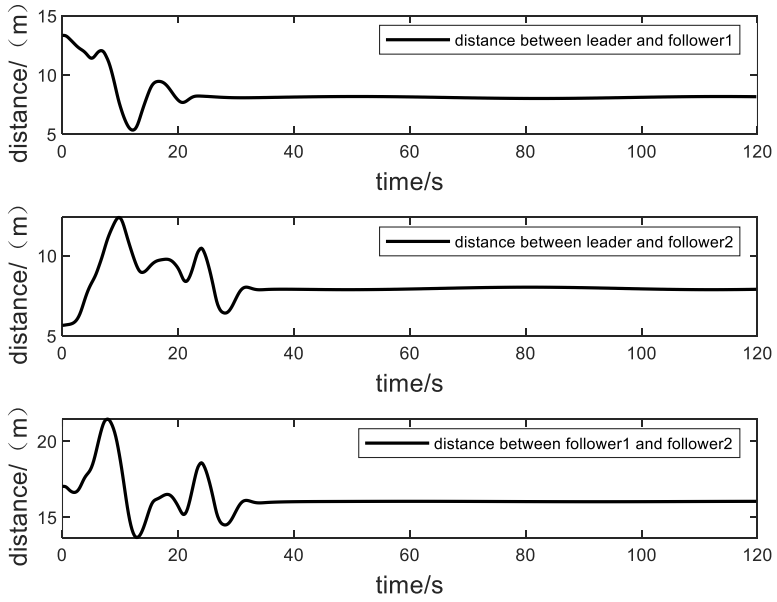

Figure 17.Graph of the change in distance between two USVs(Case II)

Case III: line trajectory tracking

The expression of the desired trajectory: $x_R = 1.5t, y_R = 1.5t$.

The initial condition of the leader is $x_l = \begin{bmatrix} -5 & 5 & 0 & 0 & 0 & 0 \end{bmatrix}$. The initial condition of the first follower is $x_1 = \begin{bmatrix} -15 & 5 & 0 & 0 & 0 & 0 \end{bmatrix}$, whose formation is $L_1 = \begin{bmatrix} -5 & -5 \end{bmatrix}$. The initial condition of the second follower is $x_2 = \begin{bmatrix} -15 & 15 & 0 & 0 & 0 & 0 \end{bmatrix}$, whose formation is $L_2 = \begin{bmatrix} -5 & 5 \end{bmatrix}$. The prediction horizon is $N_p = 20$; the control horizon is $N_c = 16$; the sampling period is $T = 0.2s$. The weighting matrices of Virtual USVs are chosen as $Q = I_4$, $R = I_2$ and $\kappa = 8$. The USVs with parameters Q and R using adaptive methods and $\kappa = 1.5$.

Corresponding Author: Zaopeng Dong, E-mail: dongzaopeng@whut.edu.cn

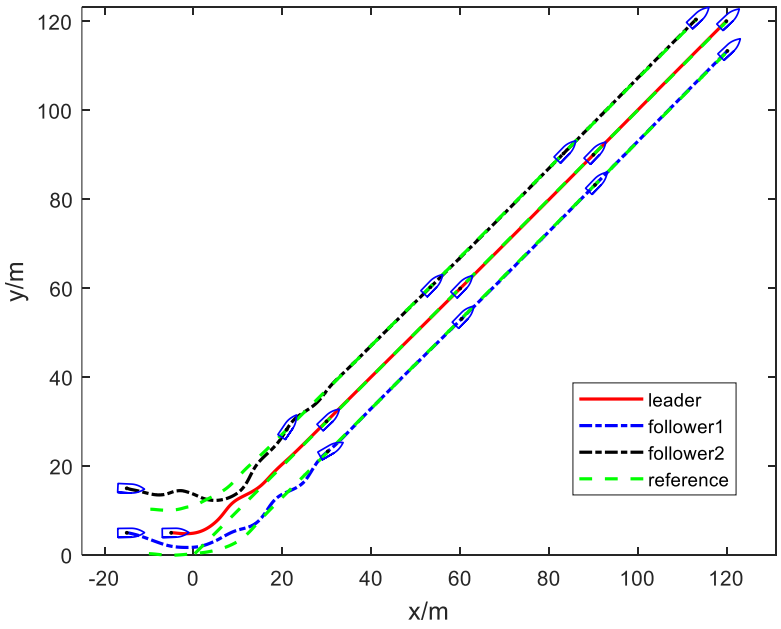

Figure 18. USVs trajectory in xoy plane(Case III)

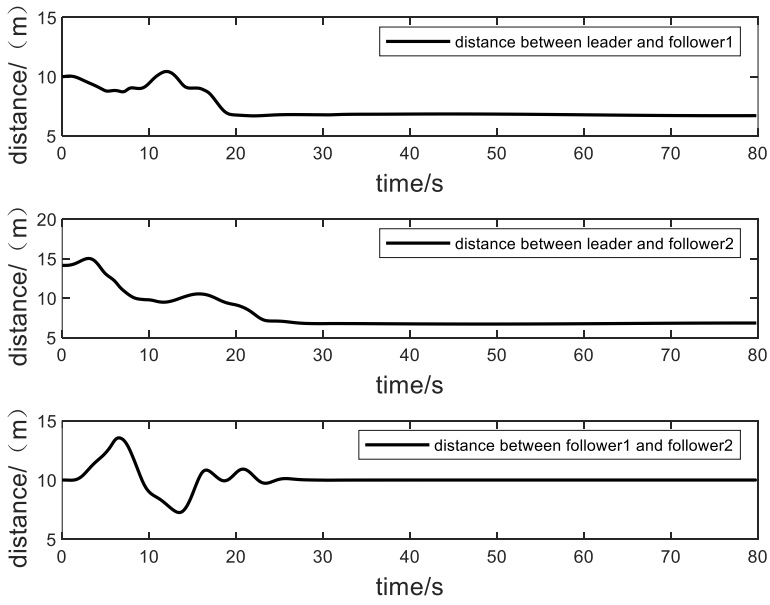

Figure 19.Graph of the change in distance between two USVs(Case III)

The effectiveness of the improved MPC method and the smoothing method of the desired trajectory are analyzed by taking the sinusoidal trajectory as an example. In which Fig.6 shows the effect of USV formation trajectory tracking after using the

Corresponding Author: Zaopeng Dong, E-mail: dongzaopeng@whut.edu.cn

improved method and using it as a control group. First, only the analysis using the improved MPC method was performed without smoothing the desired trajectories, as shown in Fig.7. Analysis of Fig. 6 and Fig. 7 reveals that the desired trajectory smoothing method has a better smoothing effect on the reference trajectory generation of the followers, and the smoothed desired trajectory affects the control effect of the USV formation. Combining with Fig.8, it can be concluded that the desired trajectory smoothing process can effectively improve the convergence speed of the USV formation.

Then, a control experiment is set up for the improved MPC method, as shown in Fig. 6 and Fig. 9, and the desired trajectory in Fig. 9 is consistent with Fig. 6. From these two trajectory plots, it is found that the fluctuation of the improved MPC trajectory is smaller compared with the traditional MPC method, where the trajectory of the leader even intersects with the trajectory of the second follower under the control of the traditional MPC method, which is very dangerous.

By analyzing Fig.10, it is found that the improved MPC under dual-mode switching has no adverse effect on its control accuracy as well as convergence speed. Further analysis of the state variable changes of the three USVs in Figs. 11 to 13 under different control methods reveals that the improved MPC has a significant effect on stabilizing the state variables. In other words, the improved controller has better control stability. Then, Fig.14 illustrates that the improved MPC controller has smoother and more energy-efficient controller inputs compared to the conventional

Corresponding Author: Zaopeng Dong, E-mail: dongzaopeng@whut.edu.cn

method.

For Case II and Case III, its simulation results are shown as Fig.16 and Fig.18. The improved control method proposed in this paper also has similar effect and can meet the requirements of USVs formation tracking control.

Seen from Fig.15, 17 and 19, it is easy to know that the three USVs maintain a safe distance from each other.

6. Conclusion

A dual model predictive control method based on virtual USV trajectory is proposed in this paper, for autonomous cooperative formation control of underactuated USVs in complex ocean environment. By designing a virtual transition trajectory to replace the actual USV's trajectory, the problem of great changes of actuators caused by large deviations in the early stage was solved. At the same time, the replacement of virtual leader USV and the introduction of improved tracking differentiator effectively smooth the expected trajectory of the follower USV, and the adaptive parameter expression designed for the weight of model predictive control parameters also improves the control effect to a certain extent. Meanwhile, the convergent speed and tracking accuracy of USV formation trajectory tracking are improved effectively by adopting the strategy of dual mode switching, and the nonlinear disturbance observer and the inherent robustness of MPC controller are combined to complete the observation and compensation of the complex marine environment disturbance. Finally, the effectiveness and reliability of the proposed

Corresponding Author: Zaopeng Dong, E-mail: dongzaopeng@whut.edu.cn

method are verified by computer simulation experiments, and all the conclusions are verified by simulation experiment results.

CRediT authorship contribution statement

Zaopeng Dong: Conceptualization, Methodology, Validation, Writing – original draft, Writing – Revised Version, Writing – review & editing, Supervision. Zhengqi Zhang: Conceptualization, Methodology, Software, Validation, Writing – original draft, Writing – review & editing. Shijie Qi: Writing – review & editing. Haisheng Zhang: Writing – review & editing. Jiakang Li: Writing – review & editing. Yuanchang Liu: Writing – review & editing, Language proofreading.

Declaration of competing interest

The authors declare that they have no known competing financial interests or personal relationships that could have appeared to influence the work reported in this paper.

Data availability

No data was used for the research described in the article.

Acknowledgments

This study was co-supported by the National Natural Science Foundation of China under Grant No.51709214 and 51779052, Science and Technology on Underwater Vehicle Laboratory under Grant No. JCKYS2022SXJQR-04, the China Postdoctoral Science Foundation funded project (No.2018M642939, 2019T120693).

Corresponding Author: Zaopeng Dong, E-mail: dongzaopeng@whut.edu.cn

References

Azarbahram, A., Pariz, N., Naghibi-Sistani, M.B., et al, 2022. Platoon of uncertain unmanned surface vehicle teams subject to stochastic environmental loads. Int. J. Adapt. Control Signal Process. 36(3), 729-750.

Baek, S., Woo, J., 2022. Model reference adaptive control-based autonomous berthing of an unmanned surface vehicle under environmental disturbance. Machines, 10(4), 244.

Bhanderi, D., McCue, L., 2020. Low cost unmanned surface vehicle swarm formation control using a potential field. Global Oceans 2020: Singapore–US Gulf Coast. IEEE, 1-4.

Chen, Y.L., Ma, X.W., Bai, G.Q., et al, 2020. Multi-autonomous underwater vehicle formation control and cluster search using a fusion control strategy at complex underwater environment. Ocean Eng. 216, 108048.

Codesseira, V.C., Tannuri, E.A., 2021. Path following control for autonomous ship using model predictive control[J]. IFAC-PapersOnLine, 54(16), 57-62.

Huang, B., Song, S., Zhu, C., et al, 2021. Finite-time distributed formation control for multiple unmanned surface vehicles with input saturation. Ocean Eng. 233, 109158.

Jiang, X., Xia, G., 2022. Sliding mode formation control of leaderless unmanned surface vehicles with environmental disturbances. Ocean Eng. 244, 110301.

Jimoh, I.A., Küçükdemiral, I.B., Bevan, G., 2021. Fin control for ship roll motion

Corresponding Author: Zaopeng Dong, E-mail: dongzaopeng@whut.edu.cn

stabilisation based on observer enhanced MPC with disturbance rate compensation. Ocean Eng. 224, 108706.

Kong, S., Sun, J., Qiu, C., et al, 2020. Extended state observer-based controller with model predictive governor for 3-d trajectory tracking of underactuated underwater vehicles. IEEE Trans. Ind. Inform. 17(9), 6114-6124.

Krell, E., King, S.A., Carrillo L.R.G, 2022. Autonomous surface vehicle energy-efficient and reward-based path planning using particle swarm optimization and visibility graphs. Appl. Ocean Res. 122, 103125.

Li, J., Du, J., Chang, W.J., 2019. Robust time-varying formation control for underactuated autonomous underwater vehicles with disturbances under input saturation. Ocean Eng. 179, 180-188.

Li, J., Du, J., Lewis, F.L., 2021. Distributed three-dimension time-varying formation control with prescribed performance for multiple underactuated autonomous underwater vehicles. Int. J. Robust Nonlinear Control. 31(13), 6272-6287.

Li, Z., Li, R., Bu, R., 2021. Path following of under-actuated ships based on model predictive control with state observer. J. Mar. Sci. Technol. 26(2), 408-418.

Liang, H., Li, H., Xu, D., 2020a. Nonlinear model predictive trajectory tracking control of underactuated marine vehicles: Theory and experiment. IEEE Trans. Ind. Electron. 68(5), 4238-4248.

Liang, Y., Li, Y., Khajepour, A., et al, 2020b. Multi-model adaptive predictive control for path following of autonomous vehicles. IET Intell. Transp. Syst. 14(14),

Corresponding Author: Zaopeng Dong, E-mail: dongzaopeng@whut.edu.cn

2092-2101.

Lindsay, J., Ross, J., Seto, M.L., et al, 2022. Collaboration of heterogeneous marine robots toward multidomain sensing and situational awareness on partially submerged targets. IEEE J. Ocean. Eng.

Liu, C., Hu, Q., Wang, X., 2021. Distributed guidance-based formation control of marine vehicles under switching topology. Appl. Ocean Res. 106, 102465.

Liu, C., Li, C., Li, W., 2020a. Computationally efficient MPC for path following of underactuated marine vessels using projection neural network. Neural Comput. Appl. 32(11), 7455-7464.

Liu, C., Wang, D., Zhang, Y., et al, 2020b. Model predictive control for path following and roll stabilization of marine vessels based on neurodynamic optimization. Ocean Eng. 217, 107524.

MahmoudZadeh, S., Abbasi, A., Yazdani, A., et al, 2022. Uninterrupted path planning system for multi-USV sampling mission in a cluttered ocean environment. Ocean Eng. 254, 111328.

Makar, A., 2022. Determination of the minimum safe distance between a USV and a hydro-engineering structure in a restricted water region sounding. Energies. 15(7), 2441.

Martinsen, A.B., Lekkas, A.M., Gros, S., 2022. Reinforcement learning-based NMPC for tracking control of ASVs: Theory and experiments. Control Eng. Practice. 120, 105024.

Corresponding Author: Zaopeng Dong, E-mail: dongzaopeng@whut.edu.cn

Meng, C., Zhang, X., 2021. Distributed leaderless formation control for multiple autonomous underwater vehicles based on adaptive nonsingular terminal sliding mode. Appl. Ocean Res. 115, 102781.

Patterson, R.G., Lawson, E., Udyawer, V., et al, 2022. Uncrewed surface vessel technological diffusion depends on cross-sectoral investment in open-ocean archetypes a systematic review of USV applications and drivers. Front. Mar. Sci. 8, 736984.

Perez, T., Fossen, T.I., 2007. Kinematic models for manoeuvring and seakeeping of marine vessels. Model. Identif. Control. 28(1), 19-30.

Rodriguez, J., Castañeda, H., Gonzalez-Garcia, A., et al, 2022. Finite-time control for an unmanned surface vehicle based on adaptive sliding mode strategy. Ocean Eng. 254, 111255.

Sandeepkumar, R., Rajendran, S., Mohan, R., et al, 2022. A unified ship manoeuvring model with a nonlinear model predictive controller for path following in regular waves. Ocean Eng. 243, 110165.

Shen, C., Shi, Y., Buckham, B., 2017. Trajectory tracking control of an autonomous underwater vehicle using Lyapunov-based model predictive control. IEEE Trans. Ind. Electron. 65(7), 5796-5805.

Shen, C., Shi, Y., 2020. Distributed implementation of nonlinear model predictive control for AUV trajectory tracking. Automatica 115, 108863.

Solnør, P., Volden, Ø., Gryte, K., et al, 2022. Hijacking of unmanned surface vehicles:

Corresponding Author: Zaopeng Dong, E-mail: dongzaopeng@whut.edu.cn

A demonstration of attacks and countermeasures in the field. J. Field Robot. 1-19.

Su, B., Wang, H., Wang, Y., 2021. Dynamic event-triggered formation control for AUVs with fixed-time integral sliding mode disturbance observer. Ocean Eng. 240, 109893.

Sun, X., Wang, G., Fan, Y., et al, 2020. A formation autonomous navigation system for unmanned surface vehicles with distributed control strategy. IEEE Trans. Intell. Transp. Syst. 22(5), 2834-2845.

Wang, H., Su, B., 2021. Event-triggered formation control of AUVs with fixed-time RBF disturbance observer. Appl. Ocean Res. 112, 102638.

Wang, J., Wang, C., Wei, Y., et al, 2019. Neuroadaptive sliding mode formation control of autonomous underwater vehicles with uncertain dynamics. IEEE Syst. J. 14(3), 3325-3333.

Wang, J., Wang, C., Wei, Y., et al, 2020. Bounded neural adaptive formation control of multiple underactuated AUVs under uncertain dynamics. ISA Trans. 105, 111-119.

Wang, W., Liu, C., 2021. An efficient ship autopilot design using observer-based model predictive control. Proc. Inst. Mech. Eng. Part M- J. Eng. Marit. Environ. 235(1), 203-212.

Wei, H., Shen, C., Shi, Y., 2019. Distributed Lyapunov-based model predictive formation tracking control for autonomous underwater vehicles subject to

Corresponding Author: Zaopeng Dong, E-mail: dongzaopeng@whut.edu.cn

disturbances. IEEE Trans. Syst. Man Cybern. -Syst. 51(8), 5198-5208.

Yan, Z., Zhang, C., Tian, W., et al, 2022. Formation trajectory tracking control of discrete-time multi-AUV in a weak communication environment. Ocean Eng. 245, 110495.

Yang, H., Deng, F., He, Y., et al, 2020. Robust nonlinear model predictive control for reference tracking of dynamic positioning ships based on nonlinear disturbance observer. Ocean Eng. 215, 107885.

Yao, X., Wang, X., Zhang, L., et al, 2020. Model predictive and adaptive neural sliding mode control for three-dimensional path following of autonomous underwater vehicle with input saturation. Neural Comput. Appl. 32(22), 16875-16889.

Zeng, Z.H., Zou, Z.J., Wang, Z.H., et al, 2020. Path following of underactuated marine vehicles based on model predictive control. Int. J. Offshore Polar Eng. 30(4), 463-470.

Zhang, Y., Liu, X., Luo, M., et al, 2019. Bio-inspired approach for long-range underwater navigation using model predictive control. IEEE T. Cybern. 51(8), 4286-4297.

Corresponding Author: Zaopeng Dong, E-mail: dongzaopeng@whut.edu.cn